博士論文

Physiological role of phosphatidylinositol selective acyltransferase LPIAT1

(ホスファチジルイノシトール特異的脂肪酸転移酵素 LPIAT1 の生理機能解析)

Takuya Kubo

久保　卓也

Contents

Abbreviation

ATGL; Adipose triglyceride lipase

CL; Cardiolipin

CoA; Coenzyme A

DHA; Docosahexaenoic acid

FADS2; Fatty acid desaturase 2

GWAS; Genome-Wide Association Study

LC3; Light Chain 3

LKO; LPIAT1 Liver specific knockout

LPIAT1; LysoPI Acyltransferase 1

MBOAT; Membrane bound O-associated Acyltransferase

NAFLD; Non-alcoholic fatty liver disease

P-407; Poloxamer 407

PAS; Periodic Acid-Schiff

PC; Phosphatidylcholine

PE; Phosphatidylethanolamine

PG; Phosphatidylglycerol

PI; Phosphatidylinositol

PI3P; Phosphatidylinositol 3-Phosphate

PIPs; Phosphatidylinositol phosphates, Phosphoinositide

PS; Phosphatidylserine

PTEN; Phosphatase and tensin homolog

PUFA; Polyunsaturated fatty acid

SM; Sphingomyelin

TAM; Tamoxifen

TG; Triglyceride

TLC; Thin-layer chromatography

Ubc; Ubiquitin c

VLDL; Very low-density lipoprotein

Vps34; Vacuolar protein sorting 34

Introduction

Polyunsaturated fatty acids (PUFAs) are required for normal function of mammalian tissues. It was reported that the lack of PUFAs causes some diseases such as sterility, ulceration, dermatitis and hepatic steatosis in nutritional and genetic studies, and PUFA supplementation can alleviate most of those symptoms [1-5].

Most fatty acids including PUFAs in cells exist in the form of phospholipids and triglycerides (TG). Biological membrane is constituted from various kinds of phospholipids. The polar head groups divide phospholipids into several classes. Not only head group classes but also the combination of different fatty acids linked to *sn* -1 and *sn* -2 positions extends the diversity. Phosphatidylinositol (PI) and phosphoinositides (PIPs), which are phosphorylated forms of PI, are unique among phospholipids in that > 60-80% of PI or PIPs has stearic acid (18:0) and arachidonic acid (20:4 n-6), which is one of the most enriched PUFAs, in several mammalian tissues including liver and brain [6-8] (Fig. 1). After *de novo* synthesized, phospholipids are metabolized by phospholipase As (deacylation) and subsequently by acyltransferases or transacylases (reacylation), termed the Lands' cycle [7,9-14].

In the *in vitro* and *in vivo* studies, specific PUFAs such as arachidonic acid (20:4 n-6) and Mead acid (20:3 n-9) are more efficiently incorporated into PI when added to culture medium or diet than other PUFAs [15-18]. These reports imply the significance of fatty acid structure of PI. Previous studies demonstrated that arachidonic acid in PI is reduced in aged rats [19], ethanol-treated rats [20-23] and

cirrhosis patients [24]. Thus dysregulation of PI acyl chains would be related to disease.

Recently, RNAi screening in *Caenorhabditis elegans* has identified the gene coding lysoPI acyltransferase [25]. The gene, named *mboa-7*, is evolutionally well conserved and there is one orthologue in mammals, LPIAT1, named for its enzymatic activity [26]. *LPIAT1*/*mboa-7* belongs to MBOAT (Membrane Bound O-Acyltransferase) family and LPIAT1 has highly specific activity for arachidonoyl-CoA and lysoPI [27,28]. In *Lpiat1*$^{-/-}$ mice, there was no LPIAT activity with arachidonoyl-CoA as an acyl donor and the content of arachidonic acid in PI was reduced [28]. *Lpiat1*$^{-/-}$ mice exhibit atrophy of the cortical cortex and hippocampus during embryonic development [28-30]. Furthermore recent genome-wide association study (GWAS) revealed variant in LPIAT1 as important risk loci for alcohol-related cirrhosis [31]. These reports suggest that LPIAT1 and its enzymatic product, arachidonoyl PI, have biologically significant roles. However, because of lethality, it was difficult to assess the role of LPIAT1and arachidonic acid-containing PI in matured adult mice. In the present study, I generated conditional *Lpiat1* knockout mice to study physiological role of LPIAT1 in adult mice.

Materials and Methods

Generation of Lpiat1 floxed mice

A ~2 kb fragment of genomic DNA containing exon 2-4 of the mouse *Lpiat1* gene was flanked by two loxP sites containing the neomycin-resistant (neo^r) cassette (Fig. 2 Mutant allele). The neo^r cassette was flanked by two FRT sites, and deleted by crossing to flippase-expressing mice (Fig. 2 Floxed allele). I used the following primers to detect wild-type *Lpiat1*and *Lpiat1 floxed* alleles: P1, 5′-CAC GCC CTT CAC CAA TGC TG-3′, P2, 5′-TGG AGG ACG GTT TGC TAC AGA CTC-3′ and deleted alleles were detected with following primers: P3, 5'-GGG TCA TAA ATG GAA GTA GAA GTA-3', P4, 5'-TCT ATA GAG TAA TTT TCC TCC TTG G-3'. *Ubc-CreER^{T2}* [32] mice and *Alb-Cre* [33] mice were obtained from The Jackson Laboratory. In *Ubc-CreER^{T2}* mice, fusion Cre recombinase-ER^{T2} protein is expressed ubiquitously under control of the human ubiquitin C (UBC) promoter and is activated by TAM or its metabolite 4-hydroxytamoxifen. In *Alb-Cre* mice, a nuclear localization sequence-modified Cre recombinase is expressed in hepatocytes under control of the mouse albumin. *Lpiat1$^{f/f}$* mice were crossed with *Ubc-CreER^{T2}* and *Alb-Cre* mice to generate *Ubc-Cre, Lpiat1$^{f/f}$* and *Alb-Cre, Lpiat1$^{f/f}$* respectively. Tamoxifen (TAM) was solubilized at a concentration of 20 mg/ml in corn oil (Wako, Japan) and 200 µl per 20 g body weight was injected intraperitoneally into 8-week-old male mice for 5days to delete *Lpiat1* gene in *Ubc-Cre Lpiat1$^{f/f}$*. Mice were maintained in our animal facility and treated in accordance with the guidelines

of the Institutional Animal Care Committee (Graduate School of Pharmaceutical Sciences, The University of Tokyo, Tokyo, Japan).

Histological studies

For paraffin-embedded sections, tissues were fixed in Bouin's fluid (picric acid / 37% formaldehyde / acetic acid = 75 / 25 / 5), dehydrated in gradually increasing concentrations of ethanol, xylene, paraffin, and then embedded in paraffin. Sections of 5 μm were prepared for H&E or Periodic acid Schiff (PAS) staining. For PAS staining, a Periodic Acid-Schiff staining kit (Muto Pure chemicals, Japan) was used. For cryosection, the tissue was embedded directly in O. C. T. compound (Sakura Finetek Japan), stored at -80 ºC, and sections were stained with Oil Red O. For staining, sections were put at room temperature, and washed with water, rinsed with 60% isopropanol, and stained with Oil Red O solution for 15 min. The sections were rinsed with 60% isopropanol, washed with water and mounted.

Cell culture and siRNA transfection

Huh-7 cells were maintained in Dulbecco's modified Eagle's medium (DMEM) supplemented with 10% fetal calf serum and 100 units/ml penicillin 100 mg/ml streptomycin, and 2 mM L-glutamine (PSG). Treatment of Bafilomycin A1 (Sigma) was at 125 nM for 4 hours and then cell proteins were harvested and subjected to western blotting. SiRNAs were transfected into Huh-7 cells with Lipofectamine^{TM} RNAiMAX (Invitrogen) according to the manufacturer's protocol. 3days later cells

were detached by treatment with trypsin and EDTA, and collected by centrifugation, and siRNAs were transfected again. A further 3 days later cells were analyzed. The final concentration of siRNA was 20 nM. A control small siRNA and human LPIAT1-targeted siRNA (sense, 5'-GCU ACU GCU ACG UGG GAA U dCdA-3' and antisense, 5'-AUU CCC ACG UAG CAG UAG C dTdG-3') were obtained from Nippon EGT (Toyama, Japan).

Total RNA isolation and quantitative real-time PCR

Total RNA from Huh-7 was extracted by using Isogen II (Nippongene, Toyama, Japan) and reverse-transcribed using the High Capacity cDNA Reverse Transcription kit (Applied biosystems, Foster City, CA). Quantitative real-time PCR was performed using SYBR Green PCR Master Mix (Takara) and Light-Cycler 480 (Roche Diagnostics). The sequences of the oligonucleotides were as follows. Human LPIAT1 forward (5'-GCCCTCCCTGATGGAGACA-3') and reverse (5'-GTAGGTGCGGTAGCGGAAGA-3'), β-actin forward (5'-ATGAAGATCAAGATCATTGCTCCTC-3') and reverse (5'-TGTCCACCTTCCAGCAGATGT-3'). Target gene expression was normalized on the basis of β-actin content.

Western blotting

Tissues from mice were homogenized in ice-cold lysis buffer (50 mM Tris-HCl pH 7.4, 150 mM NaCl, 1% TritonX-100, 0.5% sodium deoxycholate, 0.1% SDS and 20

mM EDTA) containing protease inhibitors (10 μg/ml leupeptin, 10 μg/ml pepstatin A, 10 μg/ml aprotinin, and 1 mM phenylmethylsulfonyl fluoride) by Dounce homogenizer and incubated for 10 min on ice. After centrifugation at 1,000 ×g for 20 min at 4 ºC, the supernatants were used as total protein extract. For Huh-7 analysis, cells were washed with PBS and scraped in ice cold PBS. After centrifugation, cell pellets were lysed in ice-cold lysis buffer and sonicated. Cells were centrifuged at 15,000 rpm for 10 min at 4 ºC, and the supernatants were used as total protein extract. The protein concentration was measured by the bicinchoninic acid (BCA) assay (Pierce). Each total protein extract was electrophoresed on an SDS polyacrylamide gel and transferred to PVDF membranes. Membranes were incubated with 5 or 1% (w/v) skimmed milk in TTBS buffer (10 mM Tris-HCl, pH 7.4, 150 mM NaCl, 0.05% (w/v) Tween 20) for 1 hour at room temperature, and incubated with primary antibody. The following dilutions were used: anti-LPIAT1 (1:200), anti-LC3 (1:500), anti-GAPDH (1:2000) and anti-β-actin (1:2000). Proteins were detected by enhanced chemiluminescence (ECL Western blotting detection system; GE Healthcare). Anti-LPIAT1 was generated in our laboratory [28]. Anti-LC3 was from MBL (Nagoya, Japan). Anti-GAPDH was from Calbiochem (California, USA). Anti-β-actin was from Sigma-aldrich (USA).

Lipid extraction

Lipids of each tissue and cells were extracted by the method of Bligh and Dyer [34] with some modifications. Briefly frozen tissues grinded with pestle or cells in

methanol : water : chloroform = 2 : 0.8 : 1 ml were vortexed vigorously and then 1ml of chloroform and 0.9% KCl were added. After revortexed, the mixture was centrifuged at 3000 rpm for 5 min at room temperature. The lower phase was transferred to a new tube (neutral extraction). Upper phase was added with 2 ml of chloroform and 20 μl of 1N HCl. After vortex and centrifugation, the lower phase were combined to neutral extracted solution (acidic extraction). The extracted solutions were dried up with centrifugal evaporator, dissolved in methanol : chloroform = 1 : 2, and stored at -20 ºC.

LC-ESI-Mass spectrometry analysis

The liquid chromatography-electrospray ionization mass spectrometry (LC-ESI-MS) analysis was performed by the methods previously described [35]. The liquid chromatography-electrospray ionization-tandem mass spectrometry (LC-ESI-MS/MS) analysis was performed on a Shimadzu Nexera ultra high performance liquid chromatography system (Shimadzu, Kyoto, Japan) coupled with a QTRAP 4500 hybrid triple quadrupole linear ion trap mass spectrometer (AB SCIEX, Framingham, MA, USA). Chromatographic separation was performed on an Acquity UPLC HSS T3 column (100 mm × 2.1 mm, 1.8 μm; Waters) maintained at 40 ºC using mobile phase A (water : methanol (1 : 1) containing 10 mM ammonium acetate and 0.2% acetic acid) and mobile phase B (isopropanol/acetone (1 : 1)) in a gradient program (0–3 min: 30% B→50% B; 3–24 min: 50% B→90% B; 24–28 min: 30% B) with a flow rate of 0.3 mL/min. Neutral loss scans of 74 Da with a scan

range of m/z 510-960 for Q1 in the negative ion mode were used to detect PC . Precursor ion scan of m/z 241 with a scan range of m/z 550-1000 for Q1 in the negative ion mode was used to detect PI.

Determination of phospholipid composition

Lipids were separated from total lipids by TLC on silica gel 60F254 plates (Merck) in chloroform : methanol : acetic acid = 65 : 25 : 13. The area of silica gel corresponding to each phospholipid (SM, PC, PS+PI, PE, PG, CL) was scraped off the plates. Isolated phospholipids were then extracted by the method of Bligh and Dyer described above. PS+PI fractions were further separated by TLC in chloroform : methanol : formic acid : water = 60 : 30 : 7 : 3, then PS and PI were extracted separately. To determine the amount of each phospholipid, lipid phosphorus was measured by Bartlett's method [36].

Measurement of triglyceride, cholesterol, and glycogen

For measurement of triglyceride and cholesterol, TG E Test Wako and Cholesterol E Test Wako (Wako, Japan) were used respectively. Lipid extract was dried in a glass and added 15% TritonX-100 in acetone. After dried up reaction solutions were added, incubated at 37 ºC for 10 min, and the color development was measured at 600 nm. For measurement of glycogen, Glycogen Colorimetric / Fluorometric assay kit (Biovision) were used according to manufacturer's instruction. In brief, liver homogenate or cells sonicated in water were boiled at 95 ºC for 10min to inactivate

glucosidases. After centrifugation at 18,000 ×g for 10min, supernatants were assayed. These three parameters were normalized by protein content or tissue weight.

Measurement of hepatic TG secretion rate in vivo

Measurement of hepatic TG secretion rate was performed as previous report [37] with slight modification. Mice were fasted from AM 10:00 for 6 hours and intraperitoneally injected with 200 μl of 1 mg/ml Poloxamer 407 (P-407) (Sigma) solution in sterile PBS. Blood was collected prior to injection (0 hour) and at 1.5, 4, 6 hours after injection. TG was measured with Serum Triglyceride Determination Kit (Sigma). TG secretion rate was expressed in mg/dl/hr.

Plasma lipids profile

Blood samples were collected with EDTA from the mice fasted for 6 hours. Plasma lipoprotein profiles were analyzed by an online dual enzymatic method using high-performance liquid chromatography (HPLC) (Skylight Biotech, Inc., Tokyo, Japan)

TG synthesis assay and pulse-chase assay

The siRNA treated Huh-7 cells were incubated in DMEM supplemented with 10% fetal calf serum and PSG containing and 0.4 μCi per well of [^{14}C] glycerol (0.667 nmol) for 2 or 24 hours. Then cell lipids were extracted and separated by TLC in hexane : diethyl ether : acetic acid = 70 : 30 : 1. In the case of pulse-chase assay,

after cells were incubated with [^{14}C] glycerol for 24 hours, cells were washed and chased with [^{14}C] glycerol free medium. In experiments with ATGL inhibitor, DMSO or 50 μM ATGL inhibitor was added to the medium in chase time. The radioactivity in TG normalized by protein content.

Result

Generation of *Lpiat1*deficinet mice

To circumvent neonatal lethality of *Lpiat1*-deficient mice, I generated the tamoxifen (TAM)-inducible *Lpiat1* knockout mice (*Ubc-CreER*^{T2}, *Lpiat1*$^{f/f}$) by crossing the mice carrying floxed alleles of *Lpiat1* (Fig. 2) with the mice transgenic for TAM regulated Cre recombinase fusion protein under the control of the ubiquitously expressed ubiquitin C (*Ubc*) promoter [32].

8-week-old male *Lpiat1*$^{f/f}$ mice with or without the *Cre-ER*^{T2} allele were provided with TAM, and loxP sites and *Lpiat1* gene were deleted (*Lpiat1*$^{\Delta/\Delta}$) only in the mice with *Cre-ER*^{T2} assessed by PCR 1week after the end of TAM treatment (Fig. 3A). A further 3 weeks later, LPIAT1 protein depletion was confirmed by western blotting (Fig. 3B).

Histological examination of tissues revealed that morphology of *Lpiat1*$^{\Delta/\Delta}$ brains were normal (Fig. 4), despite of the atrophy of the cerebral cortex and hippocampus in embryonic *Lpiat1* deficient mice [28]. Livers of *Lpiat1*$^{\Delta/\Delta}$ mice were apparently normal, but detailed examination revealed that cytoplasmic vacuoles in hepatocytes were observed (Fig. 5A). Kidney and spleen from *Lpiat1*$^{\Delta/\Delta}$ mice did not show apparent morphological defects.

Lpiat1 deficiency reduces total PI and 18:0/20:4-PI

I next analyzed the molecular species of phospholipids in *Lpiat1*$^{\Delta/\Delta}$ mice tissues by LC-MS. Fig. 6A shows the spectra of PI in the liver of *Lpiat1*$^{\Delta/\Delta}$ mice, and I found

that 18:0/20:4-PI was reduced to half and other species such as 18:0/18:2- and 16:0/18:1-PI were increased in comparison with *Lpiat1*$^{f/f}$ mice. It was consistent with the previous works in global Lpiat1 deficient mice [28,30]. In contrast, fatty acid composition of other major phospholipids such as PC was not affected (Fig. 6B). 18:0/20:4-PI was also reduced in other tissues such as spleen and kidney in *Lpiat1*$^{\Delta/\Delta}$ mice (Fig. 7). PI content was decreased to approximately 70% of control mice in liver (Fig. 8). These data indicate that *Lpiat1* is essential to maintain the normal PI levels and species in adult mice.

***Lpiat1* deficiency causes hepatic steatosis**

I then focused on the liver because of morphological defects (Fig. 5A). Liver sections from *Lpiat1*$^{\Delta/\Delta}$ showed intracellular vacuoles in hepatocytes, and Oil Red O staining revealed an accumulation of neutral lipids (Fig. 5B). In addition, Periodic acid Schiff (PAS) staining showed decreased glycogen content (Fig. 5C).

To investigate the cell-autonomous role of *Lpiat1* in hepatic steatosis, I next crossed the mice carrying *Lpiat1* floxed allele with the mice expressing Cre under the control hepatocyte specific albumin promoter to generate liver specific *Lpiat1* deficient mice (LKO). I confirmed the depletion of LPIAT1 protein was specific to liver in LKO mice by western blotting (Fig. 9A). Both PI level and 20:4-containing PI were decreased in LKO liver (Fig. 9B, 10). Oil red O and PAS staining revealed that increased neutral lipids and reduced glycogen storage in LKO liver (Fig. 5B, C). I measured the two major neutral lipids, triglycerides (TG) and cholesterols, and

glycogen, and found that triglyceride was increased and glycogen decreased in LKO liver (Fig. 11A, C), which was consistent with staining studies. Although the cholesterol level tends to be increased in LKO liver, a significant change was not observed in this experiment (Fig. 11B).

Liver produces very low-density lipoprotein (VLDL), which deliver TG from liver to peripheral tissues [38], and it has been reported that hepatic steatosis was developed when hepatic TG-rich VLDL secretion was inhibited [39,40]. Therefore I examined the rate of TG secretion from liver in LKO mice.

Detergent P-407, which block lipolysis of TG in VLDL by plasma lipases, has been used to determine the rate of TG secretion from liver [37] and the accumulation of TG in plasma corresponds to newly secreted TG. I injected intraperitoneally P-407 into the fasted mice and monitored TG concentration in plasma. The rate of hepatic TG secretion in LKO mice was not significantly different from that in control mice (Fig. 12). To my surprise, TG in plasma was reduced in LKO mice (Fig. 13). Although the reason for this discrepancy is unclear at present, these data suggest that the secretion defect is not the reason for development of steatosis.

LPIAT1 is required for normal TG degradation

From a kinetic standpoint, the TG accumulation in hepatocytes occurs when lipogenesis is elevated, when TG degradation or VLDL secretion is lowered [41]. However it is difficult to measure these activities directly *in vivo* except for secretion.

For this reason, I used Huh-7, a human hepatoma cell line, to study the mechanism of steatosis.

First, I treated Huh-7 cells with siRNA targeting LPIAT1, and confirmed the knockdown efficiency by quantitative real-time PCR (Fig. 14A) and western blotting (Fig. 14B). It should be noted that predominant PI species in Huh-7 is 18:0/20:3-PI instead of 18:0/20:4-PI in normal medium, and the lipid analysis showed the reduction of 18:0/20:3-PI in LPIAT1 knockdown cells (Fig. 14C). TG levels increased and glycogen levels decreased in knockdown cells (Fig. 14D, 15). Furthermore, the expression of siRNA-resistant human LPIAT1 restored TG levels and the fatty acid composition of PI (Fig. 14C, 15). These data are consistent with the results of studies *in vivo*.

Next, to determine the mechanism with which LPIAT1 regulated TG levels, I examined the activity of TG synthesis in LPIAT1 knockdown cells. Cells were incubated with [^{14}C] glycerol for 2 hours or 24 hours, and the radioactivity in TG fraction was measured (Fig. 16). I found that when cells were incubated for 2 hours, the incorporation of [^{14}C] glycerol into TG fraction was not changed in LPIAT1 knockdown cells in comparison with control cells. This result suggests that impairment of LPIAT1 didn't affect the rate of TG *de novo* synthesis. On the other hand, when cells were incubated with [^{14}C] glycerol for longer time (24 hours), the radioactivity in TG fraction was increased in LPIAT1 knockdown cells, which was consistent to an accumulation of TG.

Then, I performed pulse-chase experiments with [^{14}C] glycerol to examine whether LPIAT1 deficiency affects the rate of TG degradation. After incubation with [^{14}C] glycerol for 24 hours, cells were washed with PBS, the medium was changed to [^{14}C] glycerol-free medium and chased for 0, 2, 8 and 24 hours. I examined the radioactivity in TG at these time points and found that the radioactivity in TG was decreased to 29% at 24 hours time point relative to 0 hour time point in control cells. However, LPIAT1 knockdown cells showed a reduced the rate of TG degradation and [^{14}C] glycerol labeled TG was decreased only to 51% of its initial level (Fig. 17), indicating that LPIAT1 is required for normal TG degradation.

ATGL inhibitor further inhibits TG degradation in LPIAT1 knockdown cells

Intracellular TG is localized mainly in lipid droplets (LDs). TG in LDs is hydrolyzed either by cytosolic lipases or by lysosomal lipases. For TG degradation in lysosomes, the macroautophagy is needed to transfer cytosolic stores to lysosomes, and when macroautophagy is blocked, TG degradation is impaired. The TG degradation in the cytosol is regulated by the LD proteins such as the PAT protein family [42,43].

In many cell types including hepatocytes, ATGL (Adipose TG Lipase) is the cytosolic rate-limiting TG lipase [44]. In pulse-chase experiments, after preincubated with [^{14}C] glycerol for 24 hours, cells were incubated 8hr in the presence or absence of Atglistatin, ATGL specific inhibitor [45]. In the absence of Atglistatin, the radioactivity of TG was 59% decreased during chase incubations whereas in the

presence Atglistatin it was only 31% decreased, indicating that ATGL contributes substantially to the degradation of TG in Huh-7 cells (Fig.18). Next, I performed the pulse-chase experiments in LPIAT1 knockdown cells, in which TG degradation was inhibited (Fig. 17), and TG degradation was further inhibited in the presence of Atglistatin (Fig. 18). These results suggest that ATGL was not fully inhibited, and triglyceride lipases other than ATGL or autophagic pathway are impaired in LPIAT1 knockdown cells.

Loss of LPIAT1 causes LC3 accumulation

To test whether autophagy was blocked in LPIAT1 knockdown cells, I checked the levels of LC3-II in the presence or absence of bafilomycin A1, which inhibits the fusion of autophagosome and lysosome and impairs lysosomal degradation [46,47]. The amount of LC3-II protein was low, because autophagosomes and LC3 proteins are continuously degraded by lysosome. The increase of LC3-II protein in the presence of bafilomycin A1 indicates the amount of LC3-II that is degraded in the lysosome [48]. I used the antibody that can recognize both LC3-I and –II, although LC3-I was not detected in Huh-7. LPIAT1 knockdown cells showed increased LC3-II levels under normal conditions, and treatment of bafilomycin A1 in LPIAT1 knockdown cells showed an additional increment of the LC3-II levels with Bafilomycin A1 indicating the amounts of degraded LC3-II in LPIAT1 knockdown cells was reduced (Fig. 19A). Furthermore, I found an accumulation of LC3-I/II in

Lpiat1$^{\Delta/\Delta}$ Liver (Fig. 19B). These data suggest that autophagic flux is blocked in LPIAT1 deficient cells.

Discussion

In this study I showed that loss of LPIAT1 inhibited TG degradation, and LPIAT1 deficiency in liver leads to hepatic steatosis, the first step of NAFLD (non-alcoholic fatty liver disease). Although the precise mechanism of impairment of TG degradation remains unclear, my data imply that LPIAT1 involves lysosomal TG degradation (Fig. 18, 19). It should be noted that the impairment of autophagy also leads to increased hepatic cholesterol [42]. On the other hand, the cholesterol content in *Lpiat1* LKO liver was not accumulated although total cholesterol tended to increase (Fig. 11B). Cholesterol esters are also hydrolyzed by cytosolic cholesteryl esterases. These enzymes may be activated in LPIAT1 deficient mice. Glycogen storage was reduced in *Lpiat1* deficient liver (Fig. 5C, 11). I did not perform further analysis, and therefore the mechanism of reduced glycogen is unknown. Some lines of research suggest that glycogen breakdown is accelerated when lipolysis is impaired [49,50]. Thus, reduced glycogen storage in *Lpiat1* deficient liver may be caused by inhibition of TG degradation.

Hepatic steatosis was observed in Δ6- desaturase *Fads2* deficient mice, which is a genetic model of PUFA deficiency, and supplementation of arachidonic acids ameliorated the hepatic lipid accumulation, but supplementation of DHA did not [5]. The activation of lipogenic transcription factor SREBP1c was suggested one of the reasons for hepatic steatosis, but TG degradation activity was not examined in that report. Hepatic steatosis in *Fads2* deficient mice also may be due to impairment of TG degradation, considering my results.

My study revealed that when LPIAT1 was lost after brains fully developed, the mice showed normal morphology in brain (Fig.4), whereas the laminar structures of the cerebral cortex in embryonic LPIAT1 deficient mice were disarranged as previously reported [28]. This suggests that *Lpiat1* is not required for maintaining normal structure of brain.

PIPs are synthesized by PI kinases and phosphatases and have crucial roles in the regulation of a wide variety of cellular processes via specific interactions of PIPs-binding proteins, and dysregulation of PIPs metabolism is associated with many kinds of human diseases [51,52]. Therefore it is possible that PIPs signaling disruption in LPIAT1 deficient cells cause hepatic steatosis. Some reports demonstrated that the phosphoinositides-metabolizing enzymes were involved in the development of hepatic steatosis. One example is PTEN (Phosphatase and Tensin Homolog Deleted from Chromosome 10), which dephosphorylates $PI(3,4,5)P_3$ to generate $PI(4,5)P_2$. PTEN deficient mice exhibited severe hepatomegaly and steatosis, because of overactivation of lipogenic transcription factors (SREBP1c, PPARγ) and Akt signaling due to elevation of PIP_3 levels [53,54]. However SREBP1c and PPARγ mRNA was not elevated in *Lpiat1* LKO liver and TG synthesis was not affected by LPIAT1 knockdown in Huh-7 cells (Fig. 16), which suggests that PTEN or PIP_3 do not involve in steatosis in *Lpiat1* deficient mice. Vps34 is also associated with hepatic steatosis. When Vps34 was deleted in liver, hepatic steatosis was developed and protein turnover was inhibited [55]. The class III PI 3-kinase Vps34 generates PI3P from PI, and PI3P involves vesicular trafficking, autophagy and cytokinesis [56].

The accumulation of neutral lipids in Vps34 deficient liver is likely due to autophagy impairment. The report also showed that Vps34 deficiency in liver reduced glycogen storage. These phenotypes are similar to those in *Lpiat1* deficient mice. Thus, disruption of PI3P signaling, especially autophagic signaling, may be the major cause of hepatic steatosis in *Lpiat1* deficient mice. Our previous report showing that PI3P signaling is impaired in *mboa-7* mutants supports this hypothesis. In *C. elegans*, *mboa-7* mutants showed abnormal early endosomal morphology and caused increased LGG-1:: GFP puncta in seam cells, which is used as an autophagosome marker [57]. Another group reports that knockdown of *mboa-7* leads to increased lethality of treatment with the pathogen *Pseudomonas aeruginosa*, likely due to impaired mitophagy, a form of autophagy where defective mitochondria are selectively degraded [58]. These reports suggest that PI3P signaling is lowered when *mboa-7* gene function is disrupted.

PI is a precursor of PIPs and it is possible that some PIPs are reduced because of PI reduction in *Lpiat1*$^{\Delta/\Delta}$ and LKO (Fig. 7,9). Indeed another group have demonstrated that liver in *Lpiat1* deficient mice decreased PIP_2 with ESI-MS/MS [30]. It should be noted that the major classes of PI monophosphate is PI4P, and PI3P level is relatively low in most cells, so it is difficult to estimate the changes in PI3P levels with ESI-MS/MS. If PIPs levels are reduced as a result of dysregulation of phosphoinositides-metabolizing enzymes, the effectors will not function properly. Interestingly Shirouchi and colleagues reported that dietary PI prevented the development of NAFLD in Zucker rats [59,60]. The rats fed with PI increased liver

microsomal PI and had elevated β-oxidation activity although no change in fatty acid synthetic activity *in vitro*. Thus, total level of PI may affect lipid metabolism.

In the other hand it is possible that the altered fatty acid composition affect PIPs functions. Previous *in vitro* assay showed rat brain and liver microsomes have lysoPI acyltransferase activity but don't have lysoPIP or lysoPIP$_2$ acyltransferase activities [61], and it is thought in general that PIPs fatty acid composition is almost the same to PI fatty acid composition and reduced arachidonic acid in PI can change the fatty acid composition of PIPs [28] whereas some PIPs kinases and phosphatases have fatty acid selectivity of substrates [62].

It is likely that specific acyl chains in PIPs are required for the physiological functions in addition to their total levels. Some proteins containing PIPs-binding domain have been shown to directly interact with not only the head group but also acyl chains of PIPs *in vitro*. For example, FYVE domain of yeast Vps27p [63] and human EEA1 [64,65] have membrane insertion-residues and substitution of them significantly decreases the affinity to PI3P containing membrane. The reduced 20:4-containing PI in LPIAT1 deficient cells may lower the affinity of FYVE domain to PI3P.

Another example of the PIPs effectors that could interact with acyl chains in PIPs is α-actinin, which is the major F-actin crosslinking protein. This protein functions as a dimmer and is regulated by PIP$_2$ *in vitro* and *in vivo* [66-69]. The study of crystal structure of human α-actinin-3 actin binding domain suggests that acyl chains of PIP$_2$ disrupt the interaction between linker region of one subunit and the calmodulin-like

domain of the opposite subunit, which increased binding of α-actinin to F-actin [70]. Recent reports show that PIP_2 and PIP_3 can bind to the nuclear receptor SF-1 as ligands [71,72]. It is suggested that acyl chains of PIP_2 and PIP_3 are inserted into the hydrophobic pockets of SF-1, and IMPK modulates the gene expression under the control of SF-1 by phosphorylation of exposed head group of PIP_2. It is also possible that LPIAT1 affect the function of PIPs in cytosol or nucleus.

Acyl chains in phospholipids can function in other ways. The lateral distribution of phospholipids in biological membrane is dependent on their acyl chains and phospholipids with saturated acyl chain will form more highly ordered domains than unsaturated phospholipids [73]. Recent report shows that $PI(4,5)P_2$ is highly concentrated in caveolae and clathrin coated pit, both of which are the kind of membrane nanodomains [74]. Reduced 20:4-containing PI may alter the localization of PIPs in membrane and disrupt the downstream signaling in LPIAT1 deficient cells.

Although further studies are needed to clarify the precise molecular mechanism of inhibition of TG degradation, I revealed a new role of 20:4-containing PI in hepatic lipid metabolism.

(A)

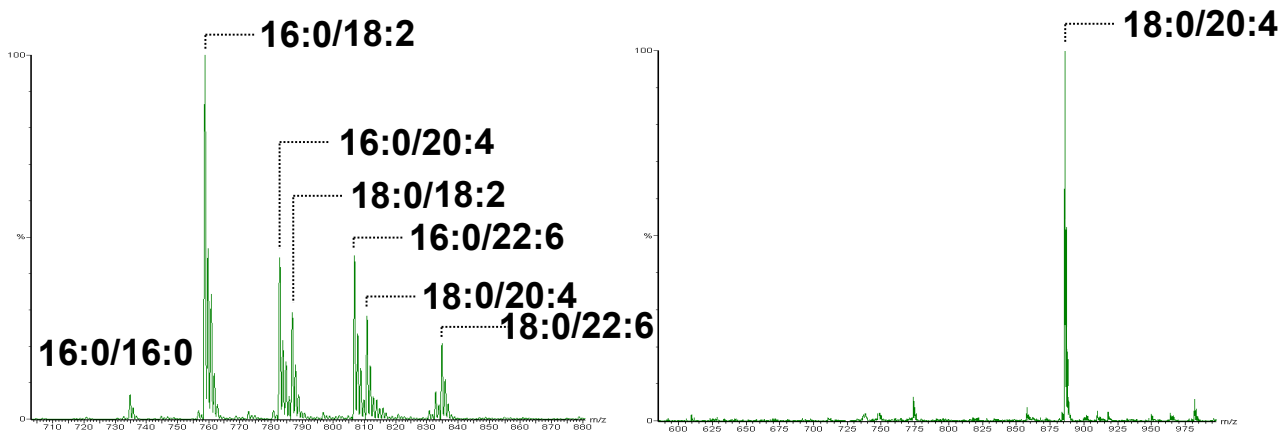

(B)

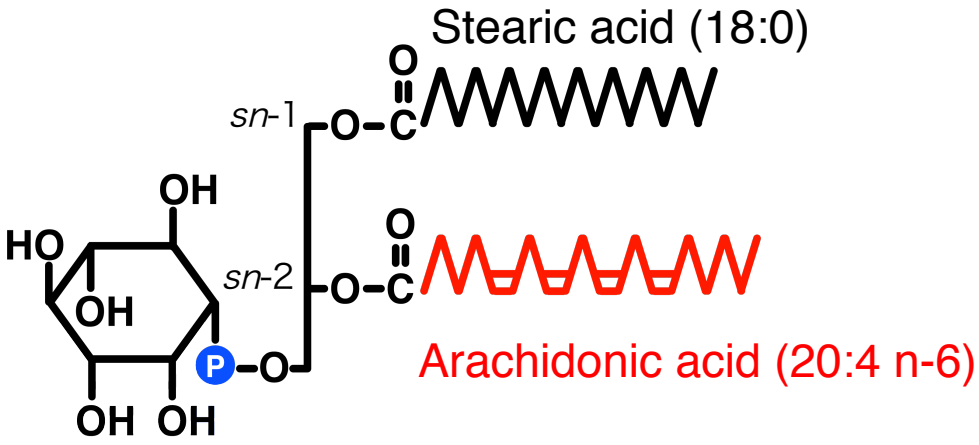

Figure 1. Unique fatty acid composition of PI
(A) Fatty acid composition of PC and PI of mouse liver analyzed by MS. (B) PI is predominatly composed of stearic acid (18:0) at the *sn*-1 position and arachidonic acid (20:4) at the *sn*-2 position.

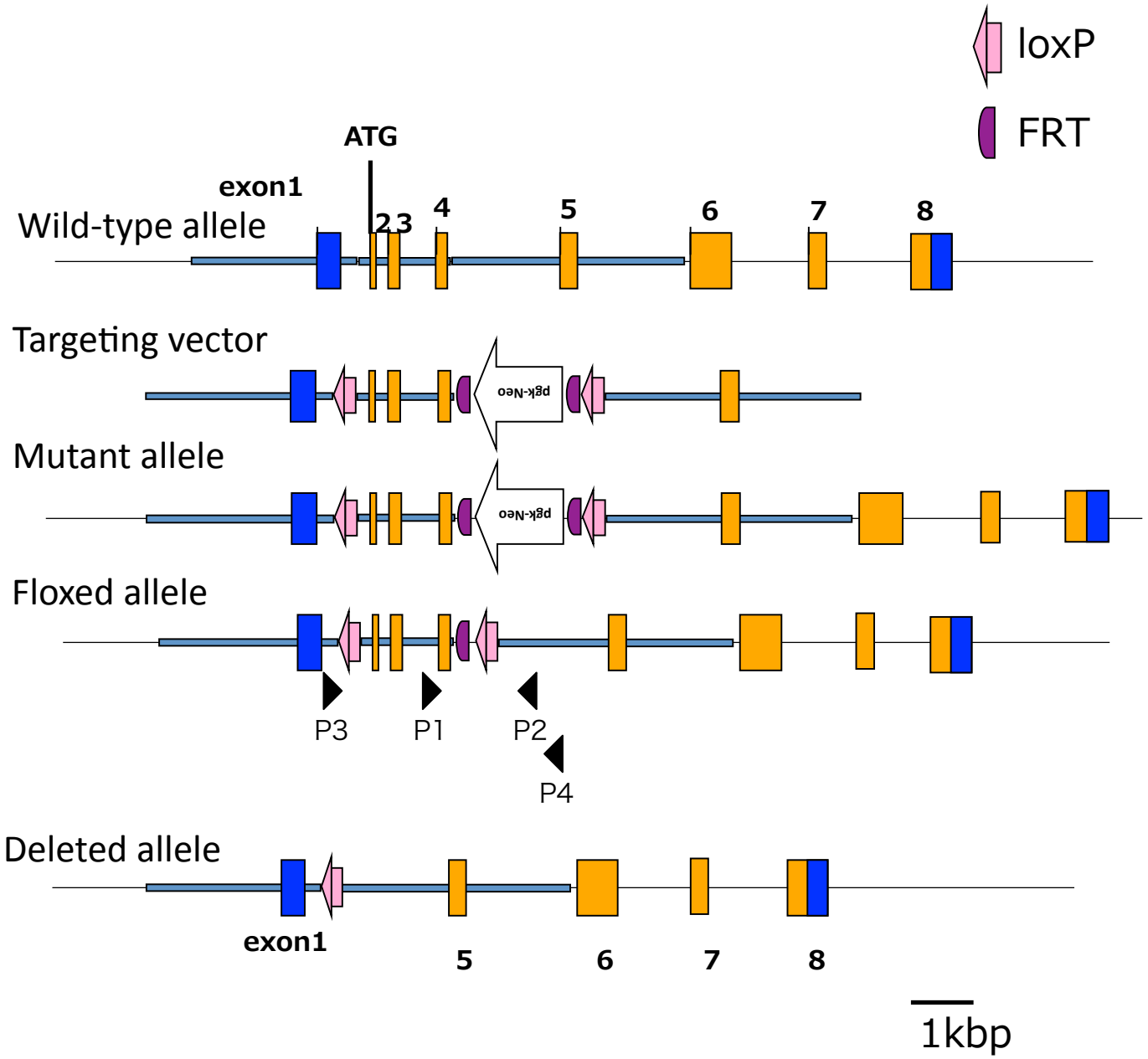

Figure 2. Generation of conditional *Lpiat1* deficient mice
Diagrams of the *Lpiat1* genomic locus and the targeting vector. The positions of PCR primers are indicated (P1, P2, P3 and P4) under the diagram of Floxed allele. The mice carrying Floxed allele and deleted allele homozygously in whole bodies are shown as *Lpiat1*$^{f/f}$ and *Lpiat1*$^{\Delta/\Delta}$ respectively. Liver-specific *Lpiat1* deleted mice are shown as LKO.

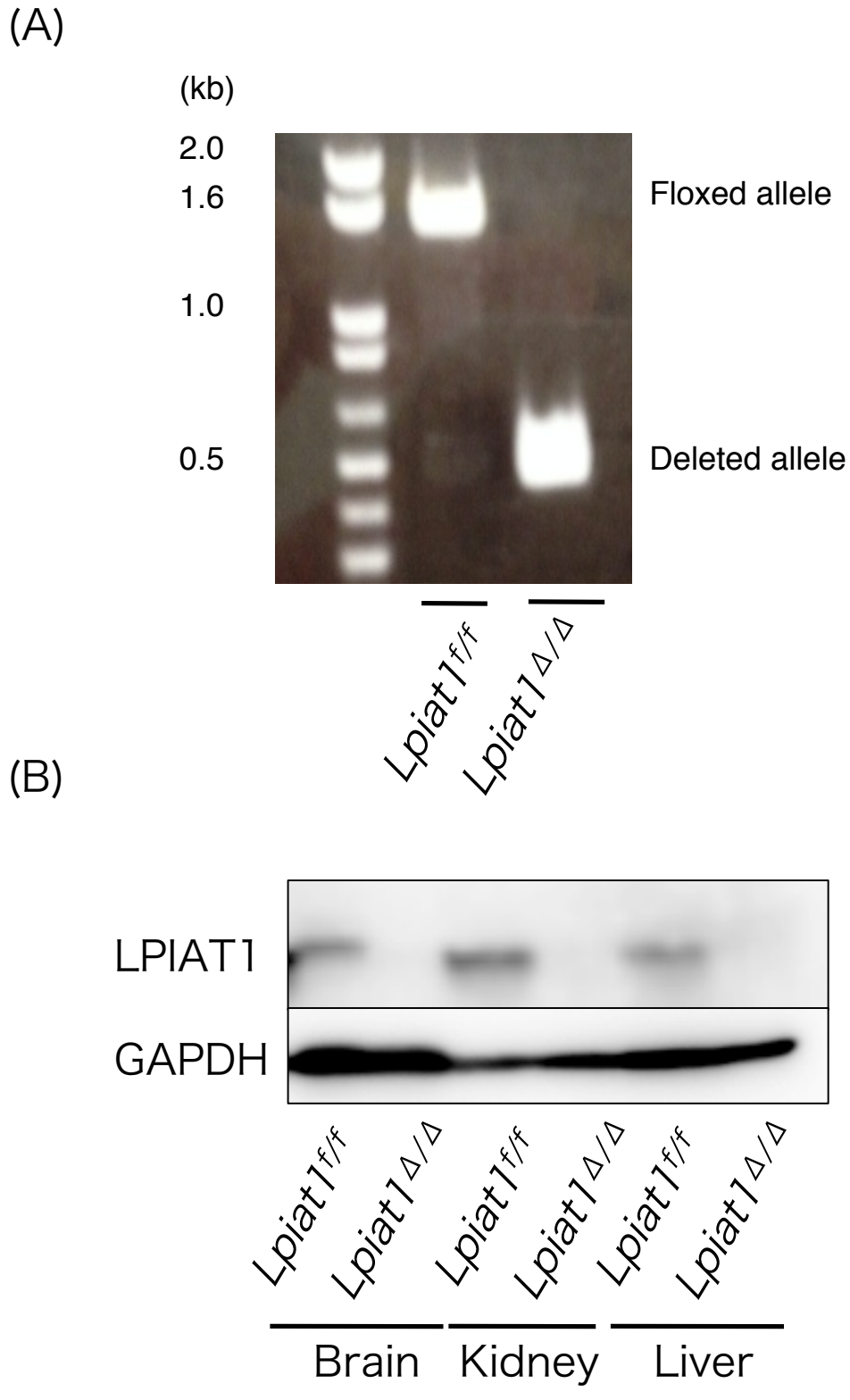

Figure 3. Deletion of LPIAT1 in mice tissue.
(A) PCR analysis for LPIAT1 deletion.
(B) Western blotting analysis of LPIAT1. Each tissue was prepared from *Lpiat1*$^{f/f}$ and *Lpiat1*$^{\Delta/\Delta}$ 4-weeks after introduction of tamoxifen.

(A)

Lpiat1$^{f/f}$ *Lpiat1*$^{\Delta/\Delta}$

cerebral cortex
Hippocampus

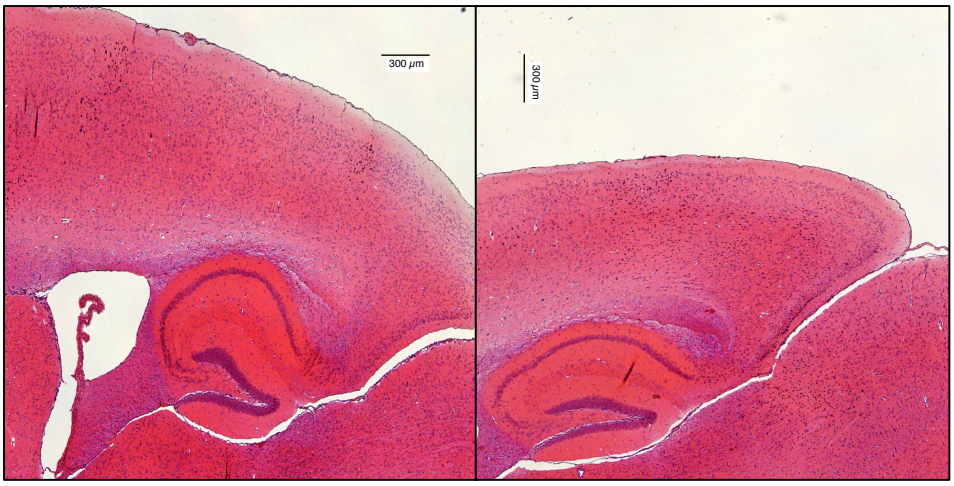

(B)

cerebellum

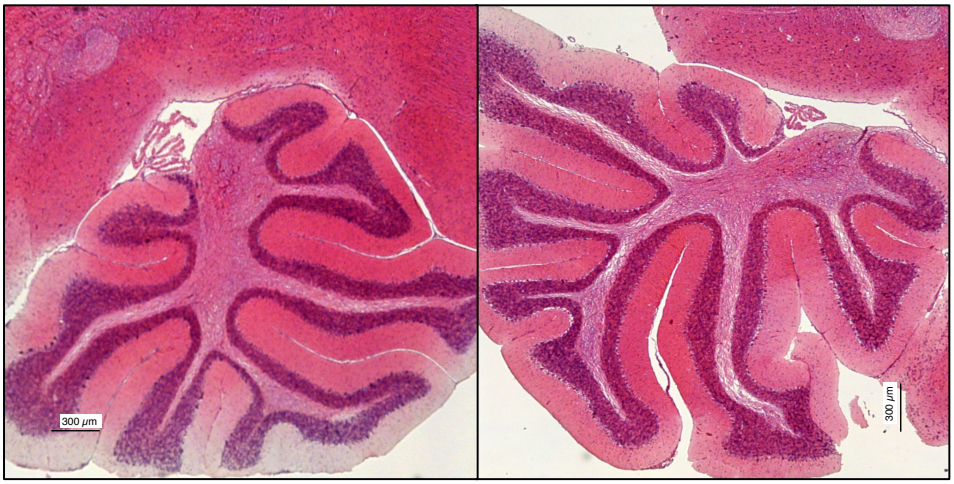

Figure 4. *Lpiat1*$^{\Delta/\Delta}$ mice brain display normal morphology
H&E staining sections of cerebral cortex, hippocampus (A) and cerebellum (B) from *Lpiat1*$^{f/f}$ (left) and *Lpiat1*$^{\Delta/\Delta}$ (right).

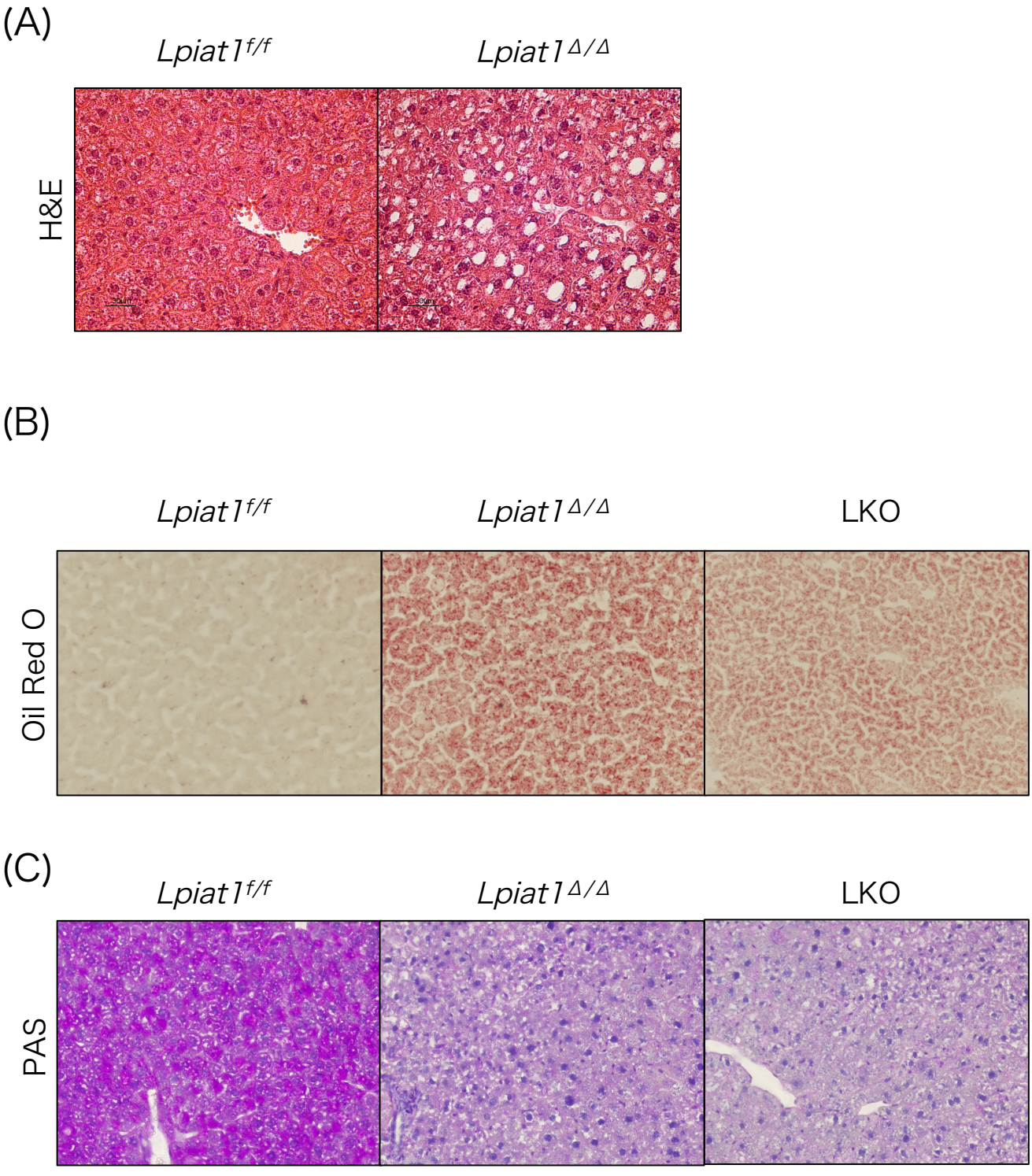

Figure 5. Hepatic steatosis and reduced glycogen storage were observed in *Lpiat1* deficient liver
Liver sections from *Lpiat1*$^{f/f}$, *Lpiat1*$^{\Delta/\Delta}$ and LKO mice stained with H&E (A), Oil Red O (B) and Periodic Acid-Schiff (C) staining.

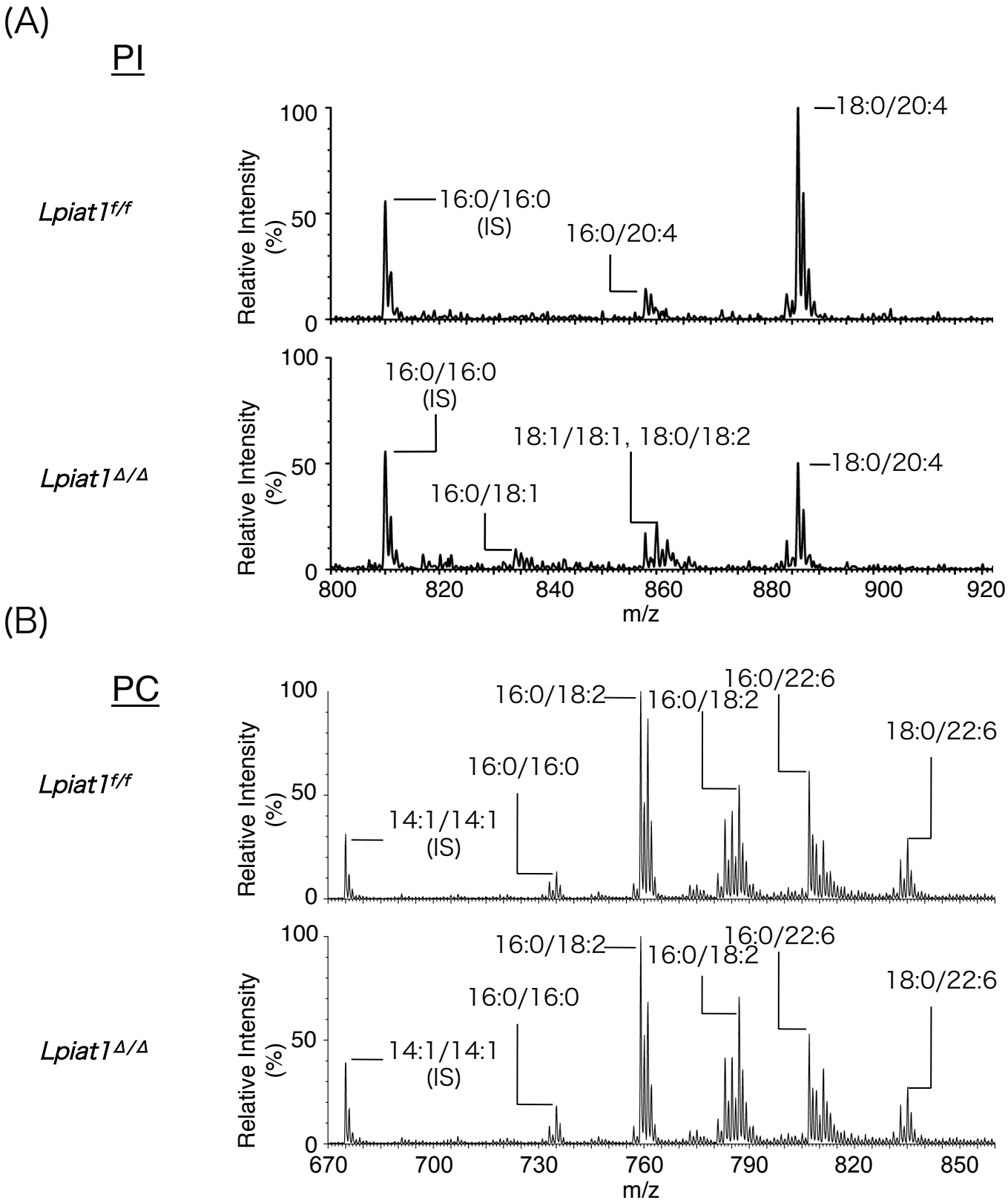

Figure 6. LC-MS spectra of phospholipids in liver
Negative ionization LC-MS spectra of PI species (A) and positive ionization spectra of PC species (B) in liver. Di-16:0 PI and di-14:1 PC are added as internal standard.

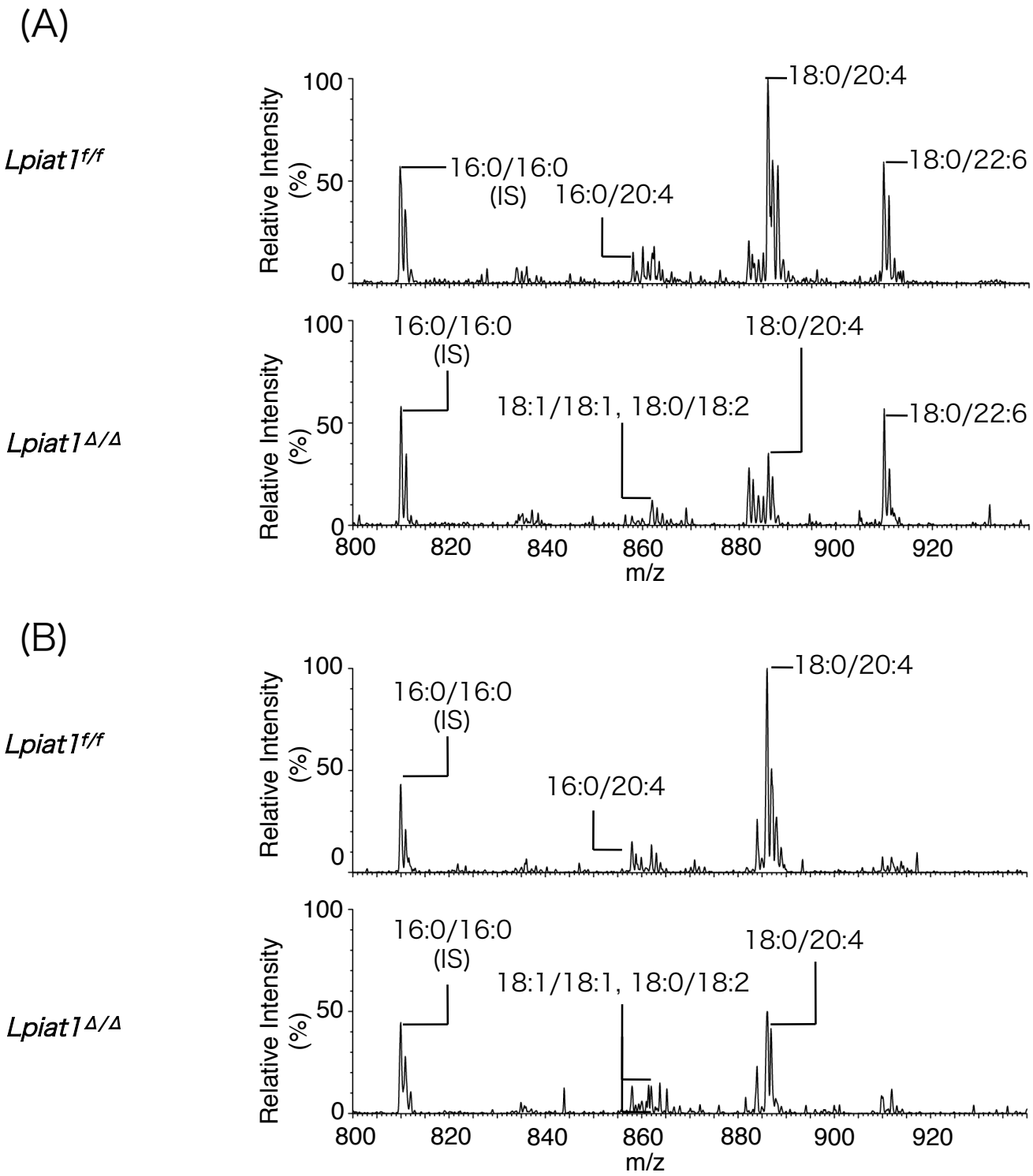

Figure 7. LC-MS spectra of PI in kidney and spleen
Negative ionization LC-MS spectra of PI species in kidney (A) and spleen (B). Di-16:0 PI as internal standard.

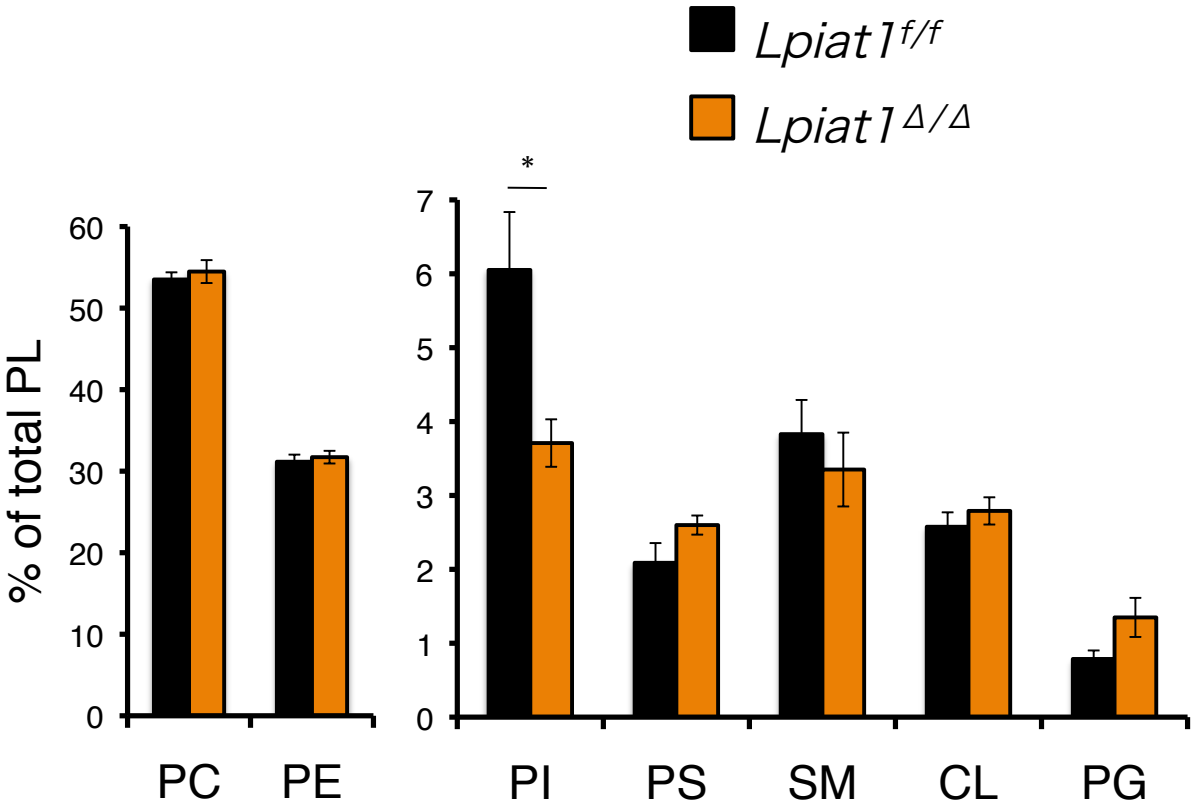

Figure 8. The content of each phospholipid in liver.
PI was reduced in *Lpiat1*$^{\Delta/\Delta}$ mice liver. Data are mean ± SEM, n = 4, *: $p < 0.05$

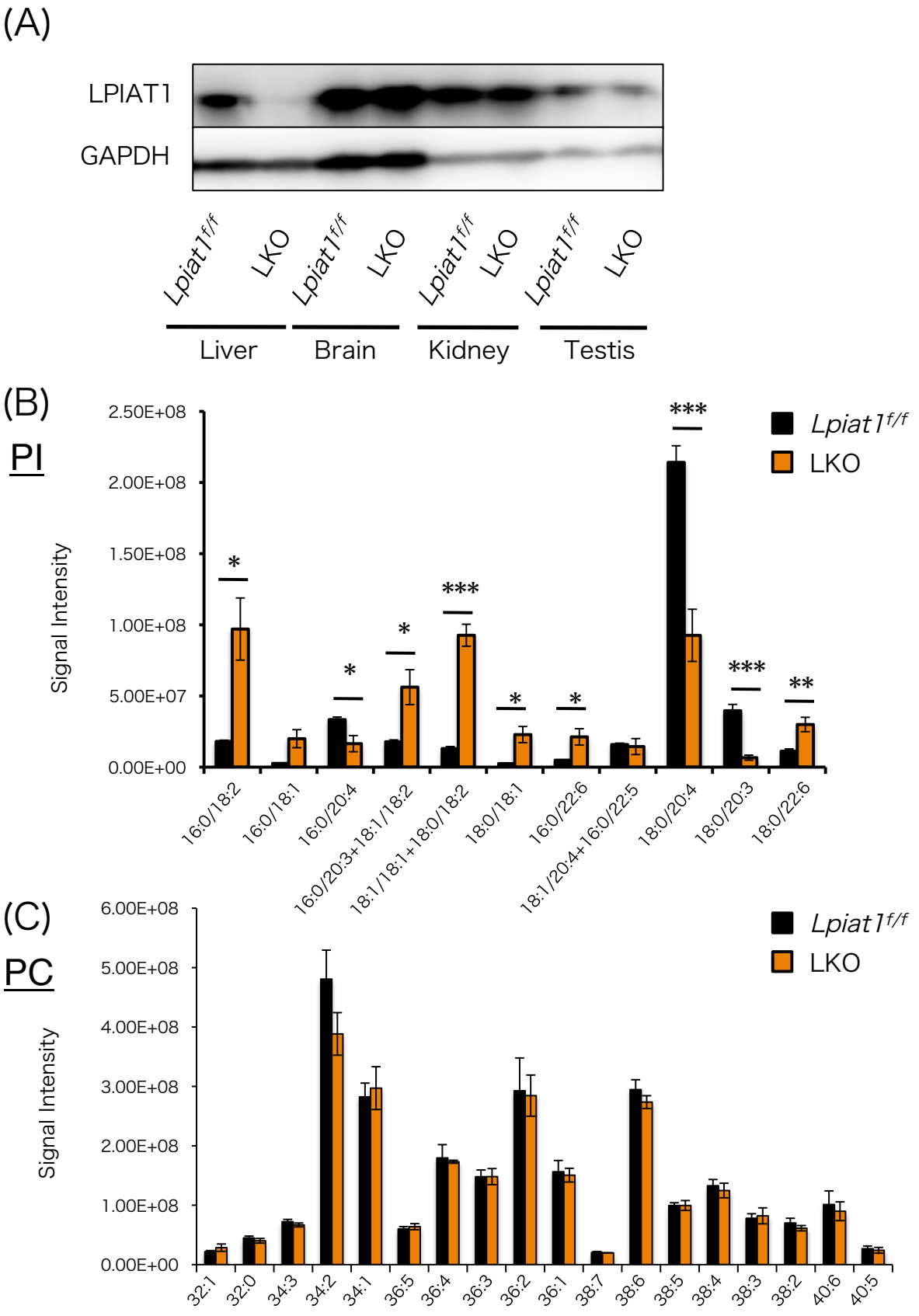

Figure 9. Liver specific *Lpiat1* deficient mice
(A) Western blotting analysis of LPIAT1. Each tissue was prepared from 12 week old male *Lpiat1*$^{f/f}$ and *Lpiat1* LKO mice.
(B, C) The signal intensity of each phospholipid species in the liver of *Lpiat1*$^{f/f}$ and LKO mice, analyzed by LC-ESI-MS/MS. (B) PI, (C) PC. Data are means ± SEM, n = 4, *: $p < 0.05$, **: $p < 0.01$, ***:$p < 0.001$

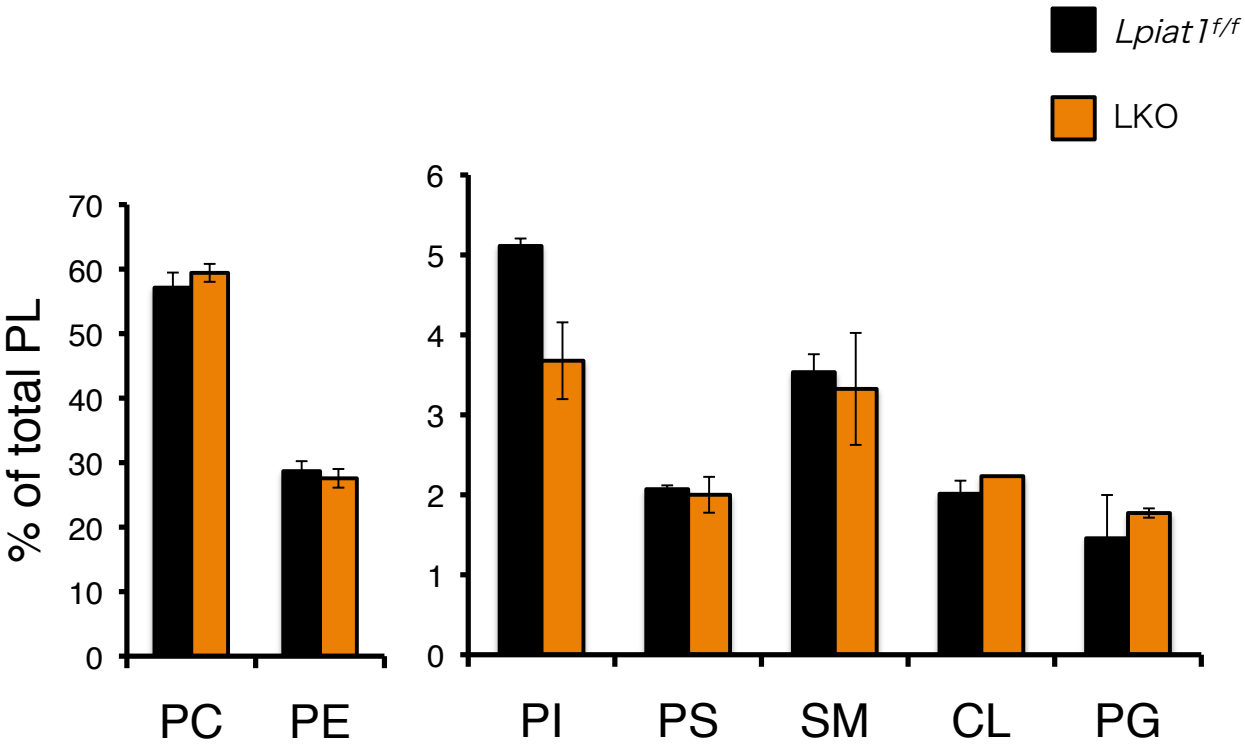

Figure 10. The content of each phospholipid in liver from *Lpiat1*$^{f/f}$ and LKO
PI was reduced in LKO mice liver. Data are mean ± SD, n = 2

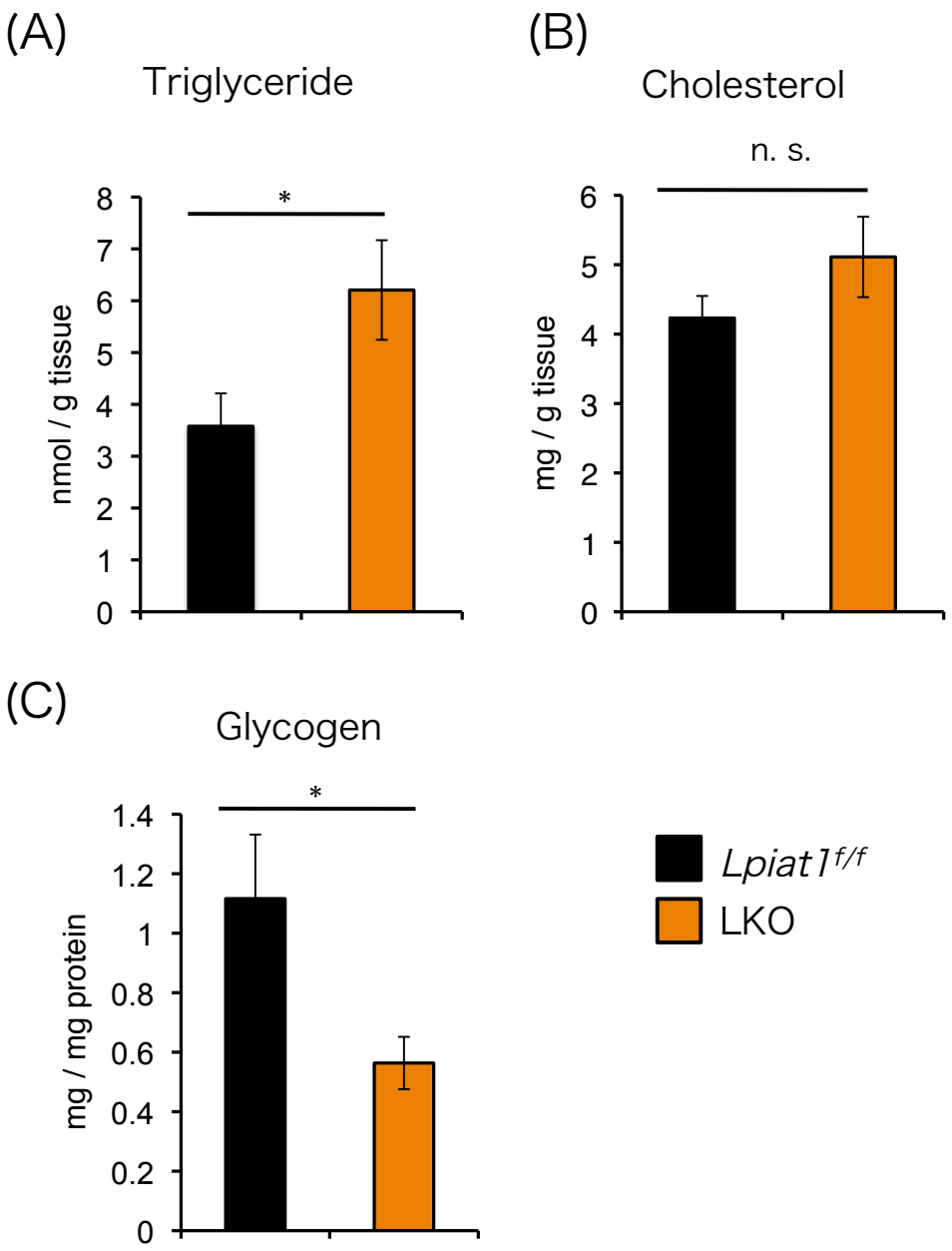

Figure 11. Total hepatic triglyceride, cholesterol and glycogen
Data are means ± SEM, n = 4 – 6, *; $p < 0.05$, n.s.; not significant

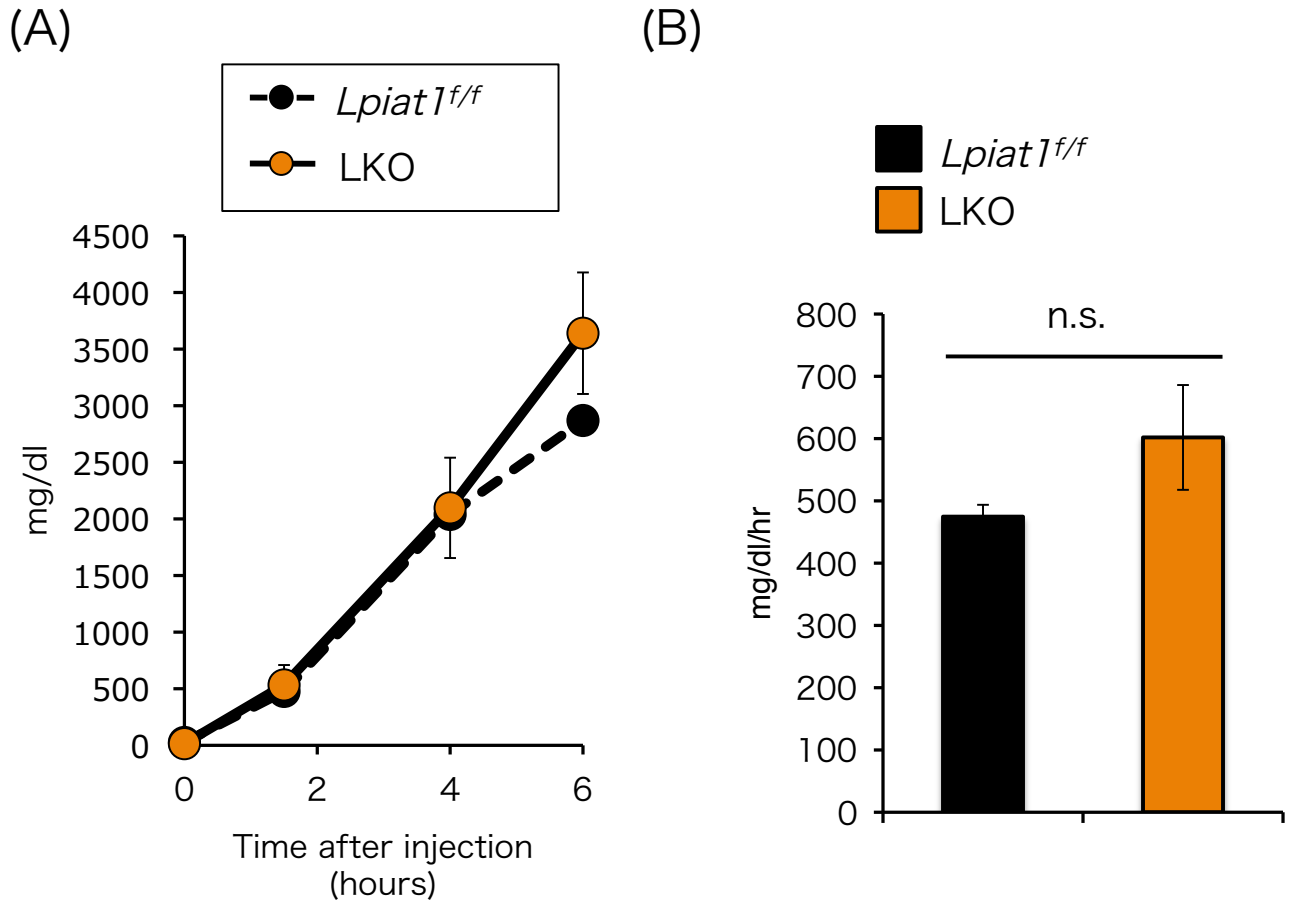

Figure 12. *In vivo* hepatic TG secretion rates
(A) The time course of TG elevation in plasma after mice injected with P-407.
(B) The rate of TG production measured from 0 to 6 hr.
Data are mean ± SEM, n = 3

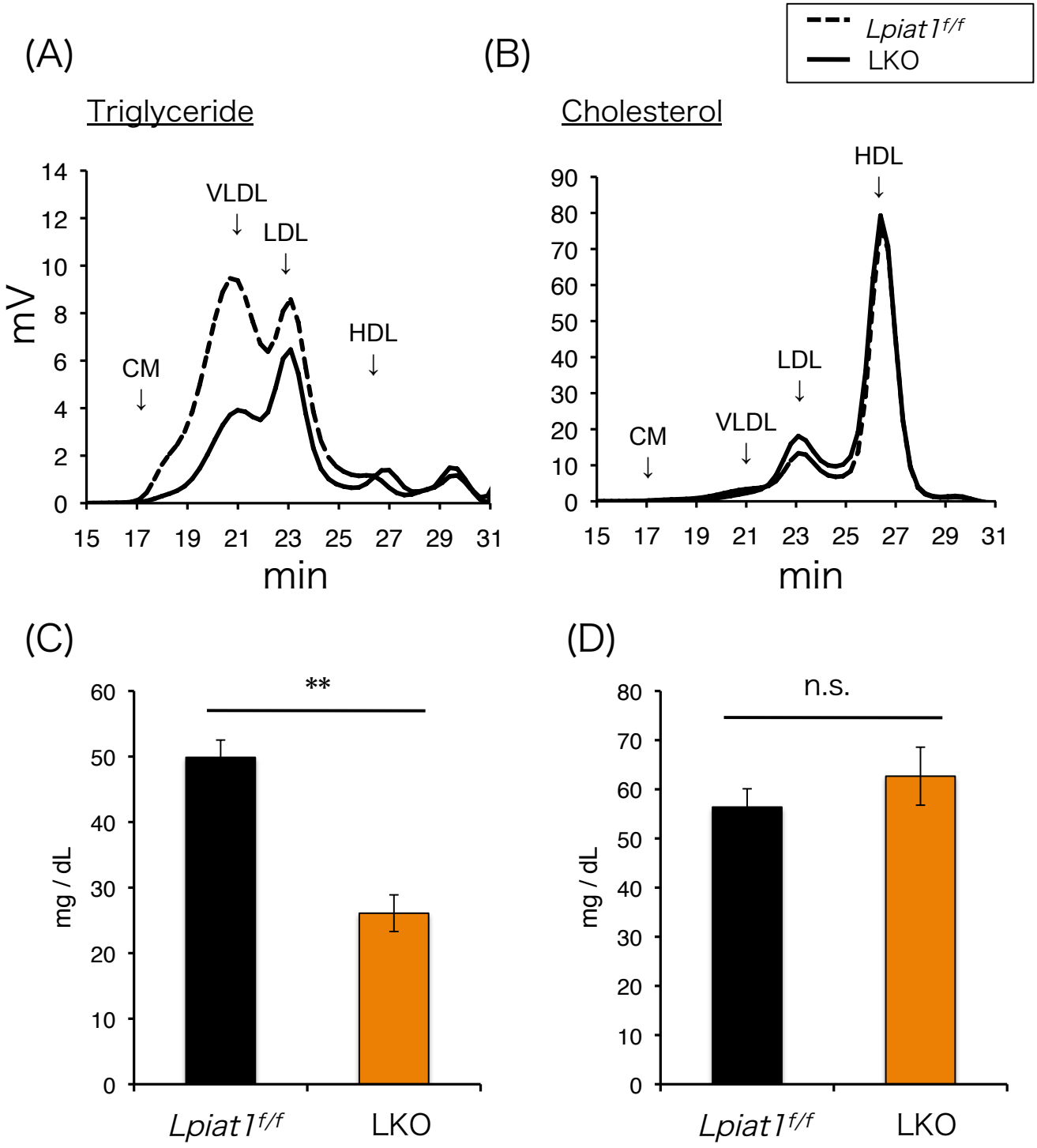

Figure 13. TG and Cholesterol in plasma
(A,B) Lipoprotein profiles in *Lpiat1*$^{f/f}$ and LKO by HPLC. TG (A) and cholesterol (B). Plasma samples were collected from 12-week-old male mice. CM; chylomicron, VLDL; very low-density lipoprotein, LDL; low-density lipoprotein, HDL; high-density lipoprotein. (C,D) total plasma Triglyceride (C) and total plasma Cholesterol (D) Data are means ± SEM, n = 3, ** : $p < 0.01$, n.s; not significant.

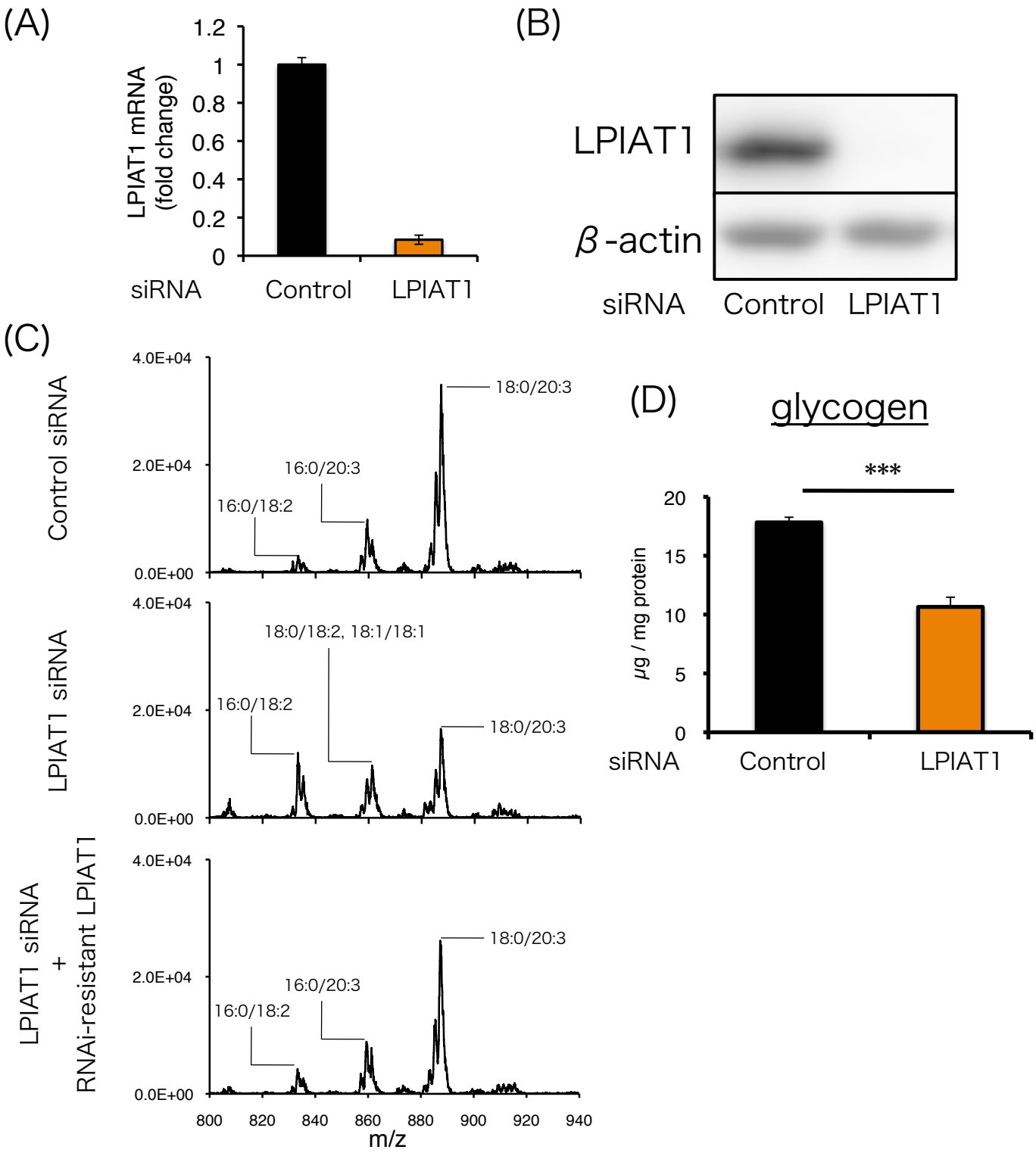

Figure 14. RNAi of LPIAT1 in Huh-7
(A, B) Huh-7 cells were transfected with siRNA targeting LPIAT1. The amount of LPIAT1 mRNA was measured by quantitative real-time PCR (A), and LPIAT1 protein was detected by western blotting (B).
(C) MS spectra of PI in Huh-7 cells. Upper, treated with control siRNA, middle, treated with LPIAT1 siRNA, lower cells expressing RNAi-resistant LPIAT1 treated with LPIAT1 siRNA
(D) glycogen content in Huh-7 . Data are means ± SEM, n = 3, *** : $p < 0.001$

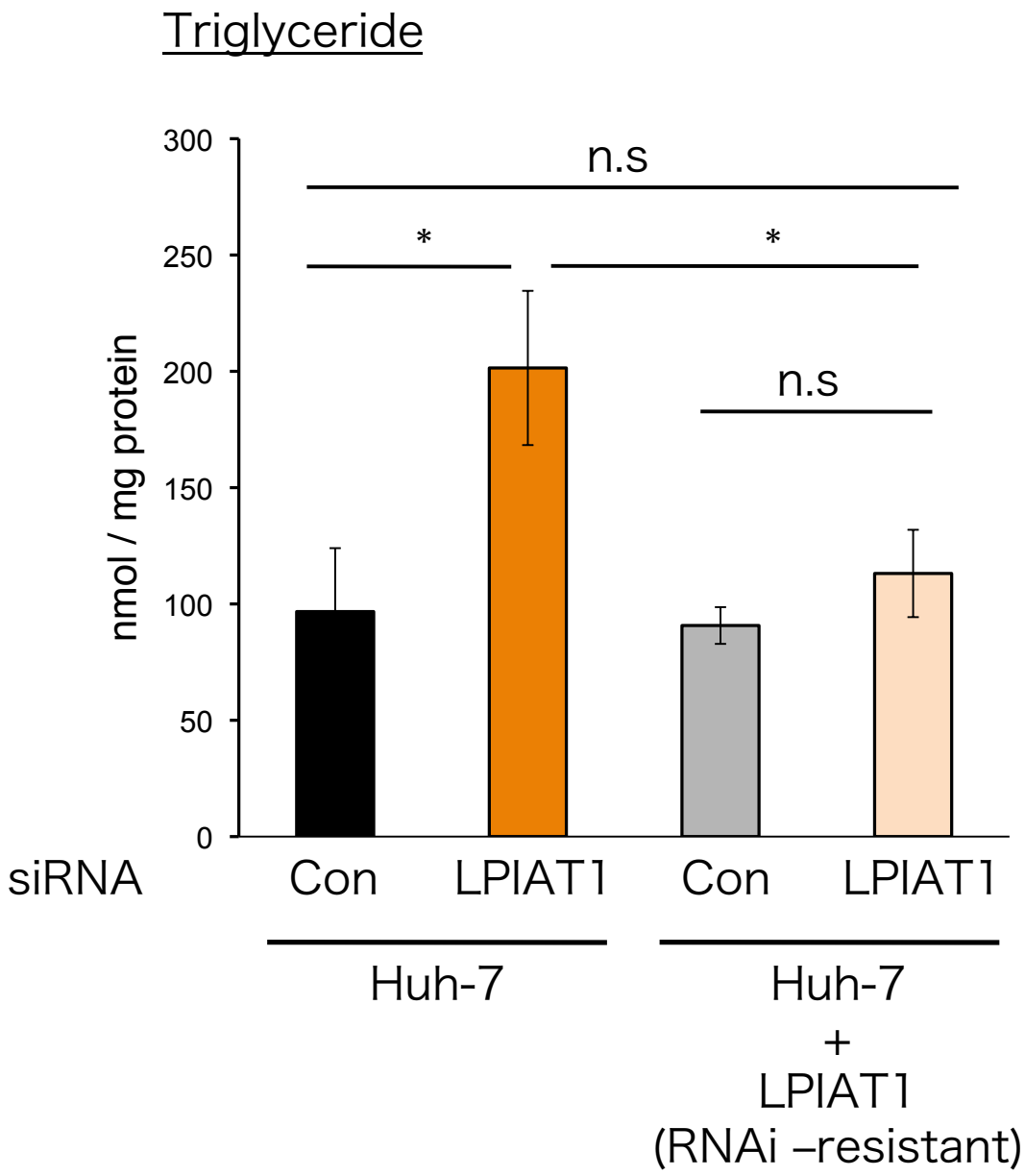

Figure 15. TG content in Huh-7 cells
Huh-7 cells and RNAi –resistant LPIAT1 expressing Huh-7 cells were transfected with siRNA and TG was measured. Data are means ± SEM, n = 3, * : $p < 0.05$, n.s; not significant. one-way ANOVA Turkey's test.

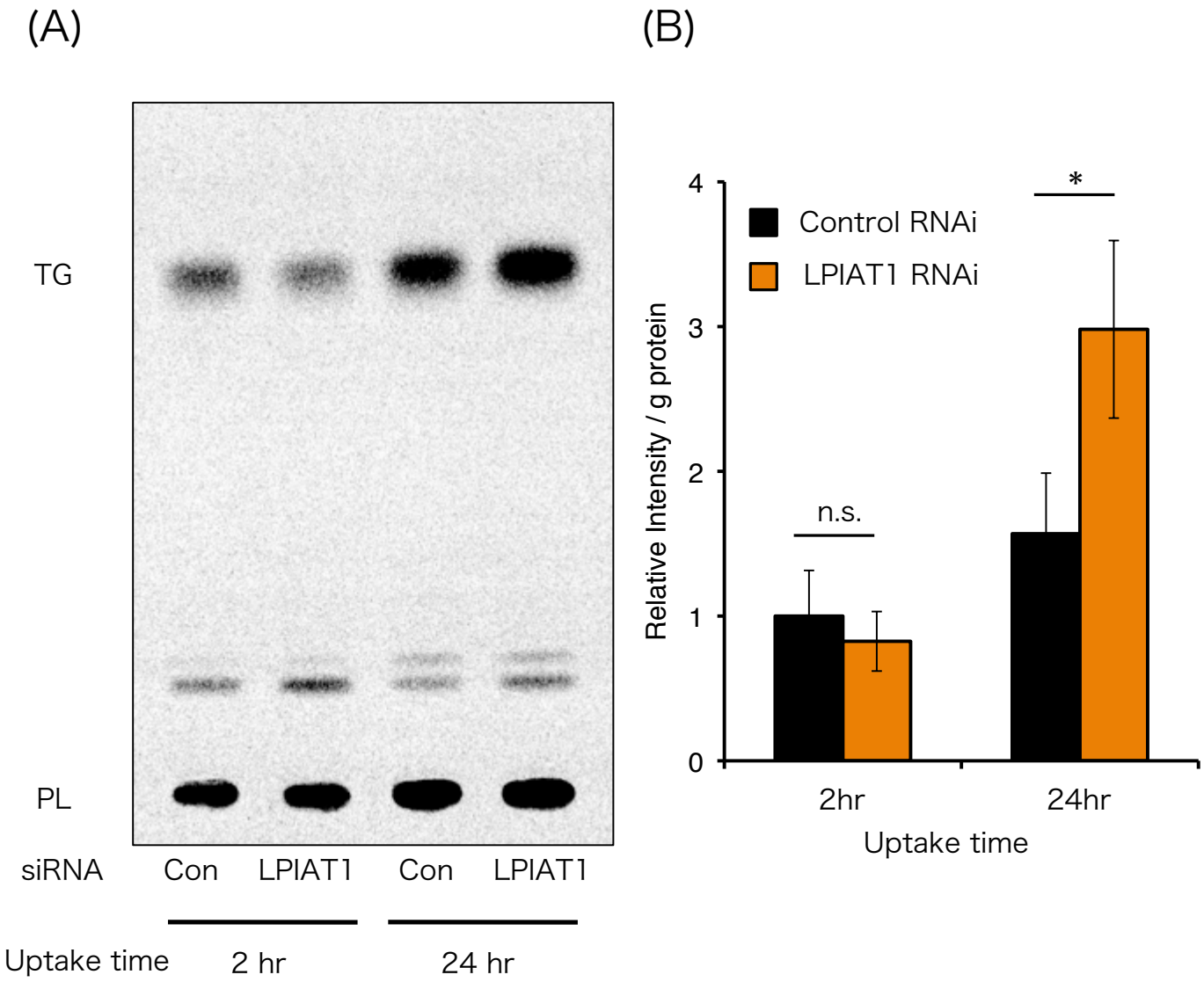

Figure 16. Incorporation of [^{14}C] glycerol to lipids in Huh-7 cells.
(A) Huh-7 cells were incubated with [^{14}C] glycerol for 2 hr or 24 hr and total lipids were separated by one-dimensional TLC.
(B) Incorporation of [^{14}C] glycerol into TG during indicated time. Data are means ± SEM, n = 3 *; $p < 0.05$, n.s.; not significant

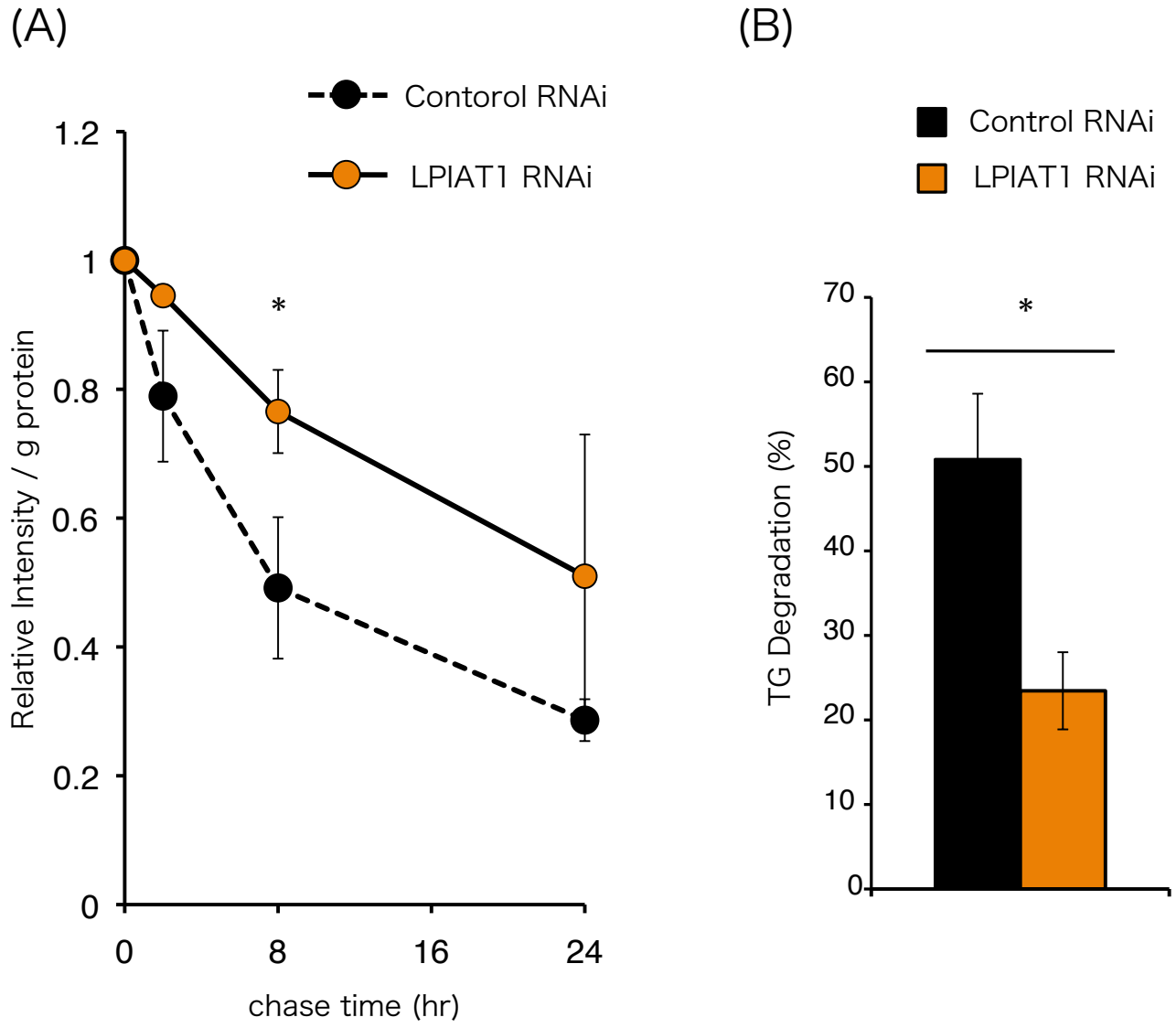

Figure 17. Impaired TG degradation by LPIAT1 knockdown
(A) Huh-7 cells were transfected with the siRNA. Cells were incubated with [^{14}C] glycerol for 24 hr and medium was replaced by [^{14}C] glycerol-free medium and chased. The time course of the radioactivity during chase were plotted.
(B) TG degradation rate at 8 hr chase compared with chase initiation time point. Data are means ± SEM, n = 3 *; $p < 0.05$

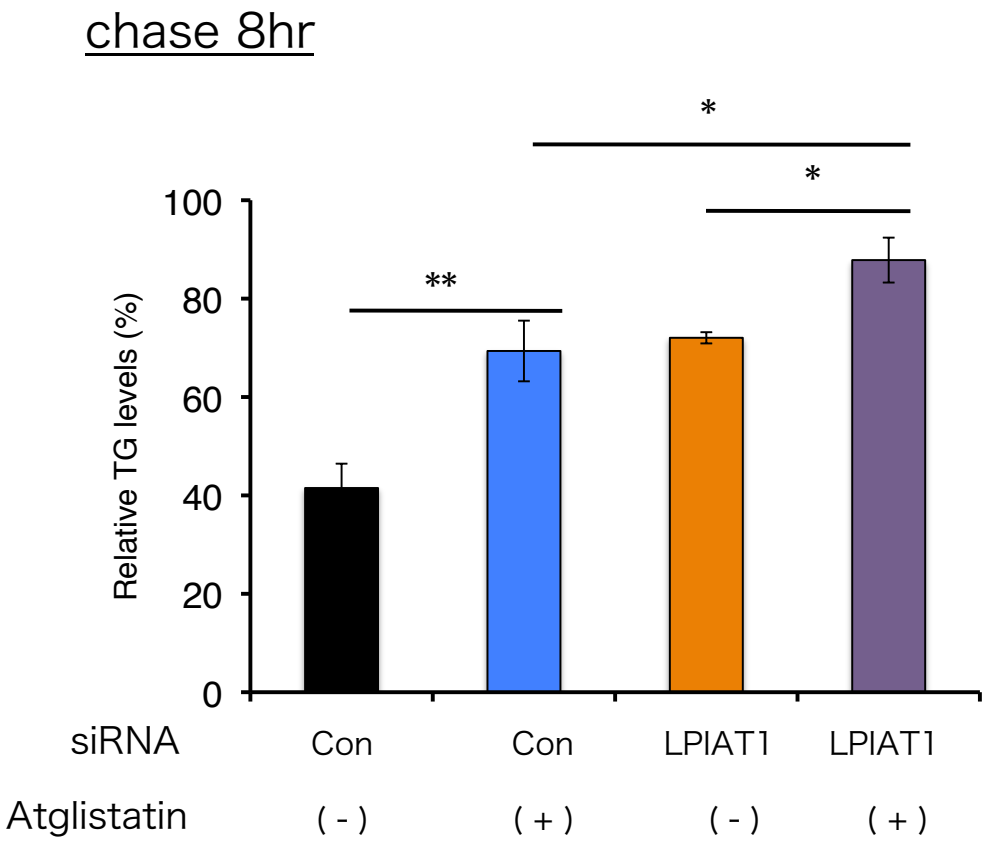

Figure 18. The effect of Atglistatin, ATGL specific inhibitor, on TG degradation
Huh-7 cells were transfected with siRNA and pulse-chase experiments were performed as Fig.17. During chase time, Atglistatin (50 μM) or DMSO was added. Mean ± SEM, n = 3 *; $p < 0.05$, **; $p < 0.01$. one-way ANOVA Turkey's test

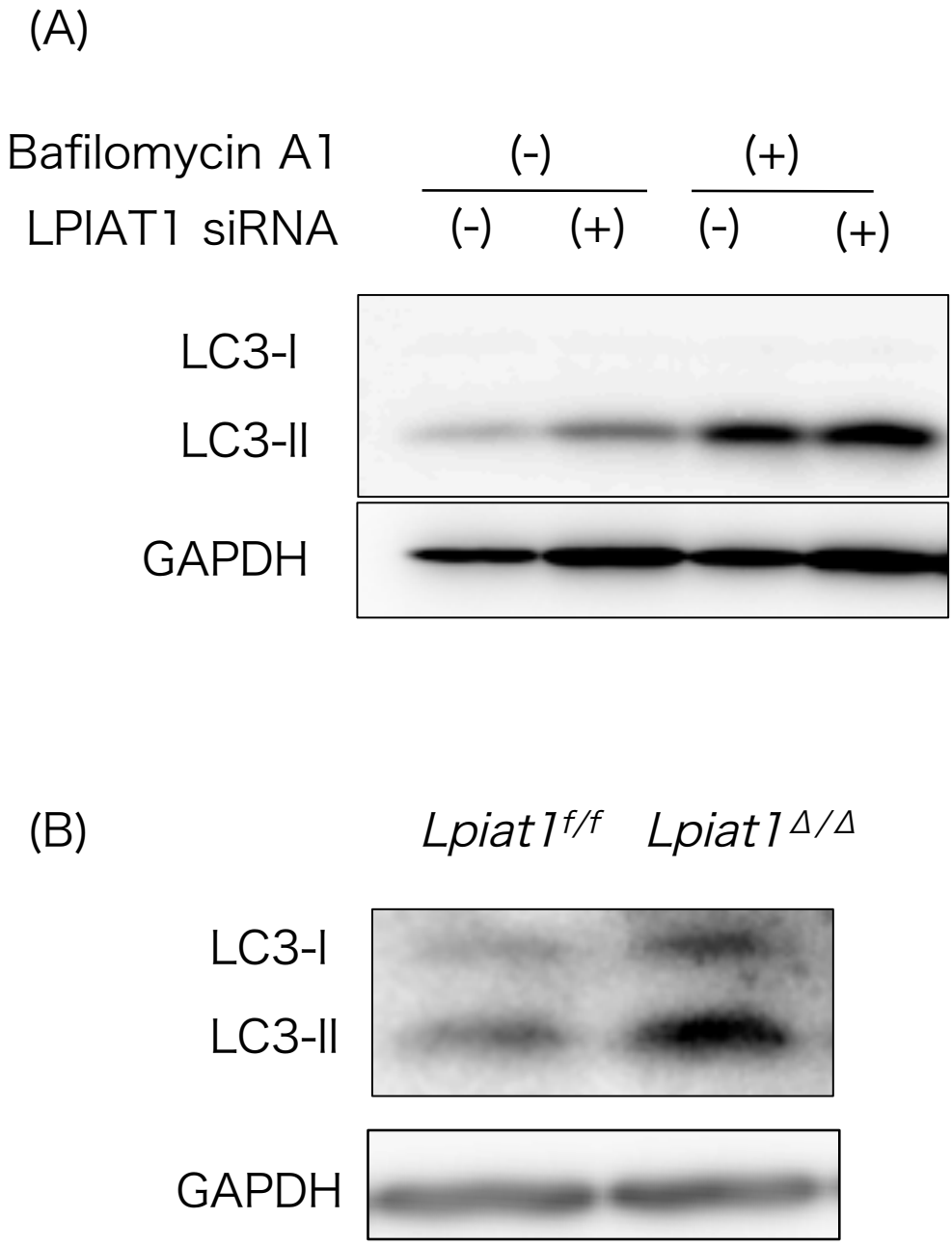

Figure 19. An accumulation of LC3 in LPIAT1 deficient cells and liver
(A) LPIAT1 knockdown Huh-7 cells or control cells were incubated in the presence or in the absence of Bafilomycin A1. Cell proteins were harvested and subjected to western blotting to detect LC3-I/II. The ratio of LC3-II to GAPDH were indicated.
(B) *Lpiat1*$^{f/f}$ and *Lpiat1*$^{\Delta/\Delta}$ mice liver were prepared for western blotting analysis of LC3-I/II.

Reference

[1] D.E. Williard, S.D. Harmon, T.L. Kaduce, M. Preuss, S.A. Moore, M.E. Robbins, et al., Docosahexaenoic acid synthesis from n-3 polyunsaturated fatty acids in differentiated rat brain astrocytes, The Journal of Lipid Research. 42 (2001) 1368–1376.

[2] C.K. Stroud, T.Y. Nara, M. Roqueta-Rivera, E.C. Radlowski, P. Lawrence, Y. Zhang, et al., Disruption of FADS2 gene in mice impairs male reproduction and causes dermal and intestinal ulceration, The Journal of Lipid Research. 50 (2009) 1870–1880. doi:10.1194/jlr.M900039-JLR200.

[3] M. Roqueta-Rivera, C.K. Stroud, W.M. Haschek, S.J. Akare, M. Segre, R.S. Brush, et al., Docosahexaenoic acid supplementation fully restores fertility and spermatogenesis in male delta-6 desaturase-null mice, The Journal of Lipid Research. 51 (2010) 360–367. doi:10.1194/jlr.M001180.

[4] W. Stoffel, B. Holz, B. Jenke, E. Binczek, R.H. Günter, C. Kiss, et al., Δ6-Desaturase (FADS2) deficiency unveils the role of ω3- and ω6-polyunsaturated fatty acids, The EMBO Journal. 27 (2008) 2281–2292. doi:10.1038/emboj.2008.156.

[5] W. Stoffel, I. Hammels, B. Jenke, E. Binczek, I. Schmidt-Soltau, S. Brodesser, et al., Obesity resistance and deregulation of lipogenesis in Δ6-fatty acid desaturase (FADS2) deficiency, EMBO Rep. 15 (2014) 110–120. doi:10.1002/embr.201338041.

[6] B.J. Holub, A. Kuksis, W. Thompson, Molecular species of mono-, di-, and triphosphoinositides of bovine brain, The Journal of Lipid Research. 11 (1970) 558–564.

[7] B.J. Holub, A. Kuksis, Differential distribution of orthophosphate- 32 P and glycerol- 14 C among molecular species of phosphatidylinositols of rat liver in vivo, The Journal of Lipid Research. 12 (1971) 699–705.

[8] R.R. Baker, W. Thompson, Positional distribution and turnover of fatty acids in phosphatidic acid, phosphinositides, phosphatidylcholine and phosphatidylethanolamine in rat brain in vivo, Biochim. Biophys. Acta. 270 (1972) 489–503.

[9] R.R. Baker, W. Thompson, Selective acylation of 1-acylglycerophosphorylinositol by rat brain microsomes. Comparison with 1-acylglycerophosphorylcholine, J. Biol. Chem. 248 (1973) 7060–7065.

[10] W.E. Lands, Metabolism of glycerolipides; a comparison of lecithin and triglyceride synthesis, J. Biol. Chem. 231 (1958) 883–888.

[11] W.E. Lands, Metabolism of glycerolipids. 2. The enzymatic acylation of lysolecithin, J. Biol. Chem. 235 (1960) 2233–2237.

[12] W.E. Lands, I. MERKL, Metabolism of glycerolipids. III. Reactivity of various acyl esters of coenzyme A with alpha'-acylglycerophosphorylcholine, and positional specificities in lecithin synthesis, J. Biol. Chem. 238 (1963) 898–904.

[13] I. MERKL, W.E. Lands, Metabolism of glycerolipids. IV. Synthesis of phosphatidylethanolamine, J. Biol. Chem. 238 (1963) 905–906.

[14] M.G. Luthra, A. Sheltawy, The metabolic turnover of molecular species of phosphatidylinositol and its precursor phosphatidic acid in guinea-pig cerebral hemispheres, J Neurochem. 27 (1976) 1501–1511.

[15] K. Retterstøl, B. Woldseth, B.O. Christophersen, Studies on the metabolism of [1-14C]5.8.11-eicosatrienoic (Mead) acid in rat hepatocytes, Biochim. Biophys. Acta. 1259 (1995) 82–88.

[16] T. Tanaka, T. Takimoto, J. Morishige, Y. Kikuta, T. Sugiura, K. Satouchi, Non-methylene-interrupted polyunsaturated fatty acids: effective substitute for arachidonate of phosphatidylinositol, Biochemical and Biophysical Research Communications. 264 (1999) 683–688. doi:10.1006/bbrc.1999.1559.

[17] T. Tanaka, J. Morishige, T. Takimoto, Y. Takai, K. Satouchi, Metabolic characterization of sciadonic acid (5c,11c,14c-eicosatrienoic acid) as an effective substitute for arachidonate of phosphatidylinositol, Eur J Biochem. 268 (2001) 4928–4939.

[18] R.L. Wolff, Structural importance of the cis-5 ethylenic bond in the endogenous desaturation product of dietary elaidic acid, cis-5,trans-9 18:2 acid, for the acylation of rat mitochondria phosphatidylinositol, Lipids. 30 (1995) 893–898.

[19] L. Ulmann, V. Mimouni, S. Roux, R. Porsolt, J.P. Poisson, Brain and hippocampus fatty acid composition in phospholipid classes of aged-relative cognitive deficit rats, Prostaglandins, Leukotrienes and Essential Fatty Acids (PLEFA). 64 (2001) 189–195. doi:10.1054/plef.2001.0260.

[20] T. Cronholm, T. Curstedt, Decrease in arachidonoyl-containing phosphatidylinositols in pancreas of rats fed an ethanol-containing diet, Biochemical Pharmacology. 33 (1984) 1105–1109.

[21] T. Cronholm, A. Neri, F. Karpe, T. Curstedt, Influence of dietary fats on pancreatic phospholipids of chronically ethanol-treated rats, Lipids. 23 (1988) 841–846. doi:10.1007/BF02536202.

[22] T.L. Smith, A.E. Vickers, K. Brendel, M.J. Gerhart, Effects of ethanol diets on cholesterol content and phospholipid acyl composition of rat hepatocytes, Lipids. 17 (1982) 124–128. doi:10.1007/BF02535091.

[23] T. Cronholm, T. Curstedt, Phosphatidylinositol composition in pancreas and submaxillary gland of ethanol-fed rats, Alcohol. 2 (1985) 183–186.

[24] D.L. Gorden, P.T. Ivanova, D.S. Myers, J.O. McIntyre, M.N. VanSaun, J.K. Wright, et al., Increased diacylglycerols characterize hepatic lipid changes in progression of human nonalcoholic fatty liver disease; comparison to a murine model, PLoS ONE. 6 (2011) e22775. doi:10.1371/journal.pone.0022775.s003.

[25] H.-C. Lee, T. Inoue, R. Imae, N. Kono, S. Shirae, S. Matsuda, et al., Caenorhabditis elegans mboa-7, a member of the MBOAT family, is required for selective incorporation of

polyunsaturated fatty acids into phosphatidylinositol, Mol. Biol. Cell. 19 (2008) 1174–1184. doi:10.1091/mbc.E07-09-0893.

[26] H. Shindou, T. Shimizu, Acyl-CoA:Lysophospholipid Acyltransferases, Journal of Biological Chemistry. 284 (2008) 1–5. doi:10.1074/jbc.R800046200.

[27] M.A. Gijón, W.R. Riekhof, S. Zarini, R.C. Murphy, D.R. Voelker, Lysophospholipid acyltransferases and arachidonate recycling in human neutrophils, J. Biol. Chem. 283 (2008) 30235–30245. doi:10.1074/jbc.M806194200.

[28] H.-C. Lee, T. Inoue, J. Sasaki, T. Kubo, S. Matsuda, Y. Nakasaki, et al., LPIAT1 regulates arachidonic acid content in phosphatidylinositol and is required for cortical lamination in mice, Mol. Biol. Cell. 23 (2012) 4689–4700. doi:10.1091/mbc.E12-09-0673.

[29] P. Vogel, R.W. Read, G.M. Hansen, B.J. Payne, D. Small, A.T. Sands, et al., Congenital hydrocephalus in genetically engineered mice, Vet. Pathol. 49 (2012) 166–181. doi:10.1177/0300985811415708.

[30] K.E. Anderson, A. Kielkowska, T.N. Durrant, V. Juvin, J. Clark, L.R. Stephens, et al., Lysophosphatidylinositol-Acyltransferase-1 (LPIAT1) Is Required to Maintain Physiological Levels of PtdIns and PtdInsP2 in the Mouse, PLoS ONE. 8 (2013) e58425. doi:10.1371/journal.pone.0058425.

[31] S. Buch, F. Stickel, E.T.E. po, M. Way, A. Herrmann, H.D. Nischalke, et al., A genome-wide association study confirms, Nat Genet. (2015) 1–8. doi:10.1038/ng.3417.

[32] Y. Ruzankina, C. Pinzon-Guzman, A. Asare, T. Ong, L. Pontano, G. Cotsarelis, et al., Deletion of the developmentally essential gene ATR in adult mice leads to age-related phenotypes and stem cell loss, Cell Stem Cell. 1 (2007) 113–126. doi:10.1016/j.stem.2007.03.002.

[33] C. Postic, M. Shiota, K.D. Niswender, T.L. Jetton, Y. Chen, J.M. Moates, et al., Dual roles for glucokinase in glucose homeostasis as determined by liver and pancreatic beta cell-specific gene knock-outs using Cre recombinase, J. Biol. Chem. 274 (1999) 305–315.

[34] E.G. BLIGH, W.J. DYER, A rapid method of total lipid extraction and purification, Can J Biochem Physiol. 37 (1959) 911–917.

[35] R. Imae, T. Inoue, M. Kimura, T. Kanamori, N.H. Tomioka, E. Kage-Nakadai, et al., Intracellular phospholipase A1 and acyltransferase, which are involved in Caenorhabditis elegans stem cell divisions, determine the sn-1 fatty acyl chain of phosphatidylinositol, Mol. Biol. Cell. 21 (2010) 3114–3124. doi:10.1091/mbc.E10-03-0195.

[36] G.R. BARTLETT, Phosphorus assay in column chromatography, J. Biol. Chem. 234 (1959) 466–468.

[37] J.S. Millar, D.A. Cromley, M.G. McCoy, D.J. Rader, J.T. Billheimer, Determining hepatic triglyceride production in mice: comparison of poloxamer 407 with Triton WR-1339, The Journal of Lipid Research. 46 (2005) 2023–2028. doi:10.1194/jlr.D500019-JLR200.

[38] G.S. Shelness, J.A. Sellers, Very-low-density lipoprotein assembly and secretion, Current Opinion in Lipidology. 12 (2001) 151–157.

[39] M. Raabe, M.M. Véniant, M.A. Sullivan, C.H. Zlot, J. Björkegren, L.B. Nielsen, et al., Analysis of the role of microsomal triglyceride transfer protein in the liver of tissue-specific knockout mice, Journal of Clinical Investigation. 103 (1999) 1287–1298. doi:10.1172/JCI6576.

[40] C.E. Chandler, D.E. Wilder, J.L. Pettini, Y.E. Savoy, S.F. Petras, G. Chang, et al., CP-346086: an MTP inhibitor that lowers plasma cholesterol and triglycerides in experimental animals and in humans, The Journal of Lipid Research. 44 (2003) 1887–1901. doi:10.1194/jlr.M300094-JLR200.

[41] Y. Kawano, D.E. Cohen, Mechanisms of hepatic triglyceride accumulation in non-alcoholic fatty liver disease, Journal of Gastroenterology. 48 (2013) 434–441. doi:10.1007/s00535-013-0758-5.

[42] R. Singh, S. Kaushik, Y. Wang, Y. Xiang, I. Novak, M. Komatsu, et al., Autophagy regulates lipid metabolism, Nature. 458 (2009) 1131–1135. doi:10.1038/nature07976.

[43] R. Zechner, R. Zimmermann, T.O. Eichmann, S.D. Kohlwein, G. Haemmerle, A. Lass, et al., FAT SIGNALS - Lipases and Lipolysis in Lipid Metabolism and Signaling, Cell Metabolism. 15 (2012) 279–291. doi:10.1016/j.cmet.2011.12.018.

[44] A. Lass, R. Zimmermann, M. Oberer, R. Zechner, Lipolysis - a highly regulated multi-enzyme complex mediates the catabolism of cellular fat stores, Progress in Lipid Research. 50 (2011) 14–27. doi:10.1016/j.plipres.2010.10.004.

[45] N. Mayer, M. Schweiger, M. Romauch, G.F. Grabner, T.O. Eichmann, E. Fuchs, et al., development of small-molecule inhibitors targeting adipose triglyceride lipase, Nat Chem Biol. 9 (2013) 785–787. doi:10.1038/nchembio.1359.

[46] A. Yamamoto, Y. Tagawa, T. Yoshimori, Y. Moriyama, R. Masaki, Y. Tashiro, Bafilomycin A1 prevents maturation of autophagic vacuoles by inhibiting fusion between autophagosomes and lysosomes in rat hepatoma cell line, H-4-II-E cells, Cell Struct. Funct. 23 (1998) 33–42.

[47] D.J. Klionsky, Z. Elazar, P.O. Seglen, D.C. Rubinsztein, Does bafilomycin A1 block the fusion of autophagosomes with lysosomes? Autophagy. 4 (2008) 849–850.

[48] N. Mizushima, T. Yoshimori, B. Levine, Methods in mammalian autophagy research, Cell. 140 (2010) 313–326. doi:10.1016/j.cell.2010.01.028.

[49] G. Karsli-Uzunbas, J.Y. Guo, S. Price, X. Teng, S.V. Laddha, S. Khor, et al., Autophagy is required for glucose homeostasis and lung tumor maintenance, Cancer Discov. 4 (2014) 914–927. doi:10.1158/2159-8290.CD-14-0363.

[50] K.T. Ong, M.T. Mashek, S.Y. Bu, D.G. Mashek, Hepatic ATGL knockdown uncouples glucose intolerance from liver TAG accumulation, The FASEB Journal. 27 (2013) 313–321. doi:10.1096/fj.12-213454.

[51] G. Di Paolo, P. De Camilli, Phosphoinositides in cell regulation and membrane dynamics, Nature. 443 (2006) 651–657. doi:10.1038/nature05185.

[52] T. Sasaki, S. Takasuga, J. Sasaki, S. Kofuji, S. Eguchi, M. Yamazaki, et al., Mammalian phosphoinositide kinases and phosphatases, Progress in Lipid Research. 48 (2009) 307–343. doi:10.1016/j.plipres.2009.06.001.

[53] Y. Horie, A. Suzuki, E. Kataoka, T. Sasaki, K. Hamada, J. Sasaki, et al., Hepatocyte-specific Pten deficiency results in steatohepatitis and hepatocellular carcinomas, Journal of Clinical Investigation. 113 (2004) 1774–1783. doi:10.1172/JCI20513DS1.

[54] B. Stiles, Y. Wang, A. Stahl, S. Bassilian, W.P. Lee, Y.-J. Kim, et al., Liver-specific deletion of negative regulator Pten results in fatty liver and insulin hypersensitivity [corrected], Proc. Natl. Acad. Sci. U.S.a. 101 (2004) 2082–2087. doi:10.1073/pnas.0308617100.

[55] N. Jaber, Z. Dou, J.-S. Chen, J. Catanzaro, Y.-P. Jiang, L.M. Ballou, et al., Class III PI3K Vps34 plays an essential role in autophagy and in heart and liver function, Proceedings of the National Academy of Sciences. 109 (2012) 2003–2008. doi:10.1073/pnas.1112848109.

[56] K.O. Schink, C. Raiborg, H. Stenmark, Phosphatidylinositol 3-phosphate, a lipid that regulates membrane dynamics, protein sorting and cell signalling, Bioessays. 35 (2013) 900–912. doi:10.1002/bies.201300064.

[57] H.-C. Lee, T. Kubo, N. Kono, E. Kage-Nakadai, K. Gengyo-Ando, S. Mitani, et al., Depletion of mboa-7, an enzyme that incorporates polyunsaturated fatty acids into phosphatidylinositol (PI), impairs PI 3-phosphate signaling in Caenorhabditis elegans, Genes to Cells. (2012). doi:10.1111/j.1365-2443.2012.01624.x.

[58] N.V. Kirienko, F.M. Ausubel, G. Ruvkun, Mitophagy confers resistance to siderophore-mediated killing by Pseudomonas aeruginosa, Proceedings of the National Academy of Sciences. (2015). doi:10.1073/pnas.1424954112.

[59] B. Shirouchi, K. Nagao, N. Inoue, K. Furuya, S. Koga, H. Matsumoto, et al., Dietary Phosphatidylinositol Prevents the Development of Nonalcoholic Fatty Liver Disease in Zucker (fa/ fa) Rats, J. Agric. Food Chem. 56 (2008) 2375–2379. doi:10.1021/jf703578d.

[60] B. Shirouchi, K. Nagao, K. Furuya, N. Inoue, M. Inafuku, M. Nasu, et al., Effect of dietary phosphatidylinositol on cholesterol metabolism in Zucker (fa/fa) rats, J Oleo Sci. 58 (2009) 111–115.

[61] F.B. Palmer, Metabolism of lysopolyphosphoinositides by rat brain and liver microsomes, Biochem. Cell Biol. 64 (1986) 117–125.

[62] K. D'Souza, R.M. Epand, Enrichment of phosphatidylinositols with specific acyl chains, Biochim. Biophys. Acta. (2013). doi:10.1016/j.bbamem.2013.10.003.

[63] S. Misra, J.H. Hurley, Crystal structure of a phosphatidylinositol 3-phosphate-specific membrane-targeting motif, the FYVE domain of Vps27p, Cell. 97 (1999) 657–666.

[64] T.G. Kutateladze, K.D. Ogburn, W.T. Watson, T. de Beer, S.D. Emr, C.G. Burd, et al., Phosphatidylinositol 3-phosphate recognition by the FYVE domain, Molecular Cell. 3 (1999) 805–811.

[65] M. Yokogawa, Y. Kobashigawa, N. Yoshida, K. Ogura, K. Harada, F. Inagaki, NMR Analyses of the Interaction between the FYVE Domain of Early Endosome Antigen 1 (EEA1) and Phosphoinositide Embedded in a Lipid Bilayer, J. Biol. Chem. 287 (2012) 34936–34945. doi:10.1074/jbc.M112.398255.

[66] T.S. Fraley, T.C. Tran, A.M. Corgan, C.A. Nash, J. Hao, D.R. Critchley, et al., Phosphoinositide binding inhibits alpha-actinin bundling activity, J. Biol. Chem. 278 (2003) 24039–24045. doi:10.1074/jbc.M213288200.

[67] T.S. Fraley, C.B. Pereira, T.C. Tran, C. Singleton, J.A. Greenwood, Phosphoinositide binding regulates alpha-actinin dynamics: mechanism for modulating cytoskeletal remodeling, J. Biol. Chem. 280 (2005) 15479–15482. doi:10.1074/jbc.M500631200.

[68] K. Fukami, T. Endo, M. Imamura, T. TAKENAWA, alpha-Actinin and vinculin are PIP2-binding proteins involved in signaling by tyrosine kinase, J. Biol. Chem. 269 (1994) 1518–1522.

[69] K. Fukami, K. Furuhashi, M. Inagaki, T. Endo, S. Hatano, T. TAKENAWA, Requirement of phosphatidylinositol 4,5-bisphosphate for alpha-actinin function, Nature. 359 (1992) 150–152. doi:10.1038/359150a0.

[70] G. Franzot, B. Sjöblom, M. Gautel, K. Djinović Carugo, The crystal structure of the actin binding domain from alpha-actinin in its closed conformation: structural insight into phospholipid regulation of alpha-actinin, Journal of Molecular Biology. 348 (2005) 151–165. doi:10.1016/j.jmb.2005.01.002.

[71] R.D. Blind, M. Suzawa, H.A. Ingraham, Direct Modification and Activation of a Nuclear Receptor-PIP2 Complex by the Inositol Lipid Kinase IPMK, Science Signaling. 5 (2012) ra44. doi:10.1126/scisignal.2003111.

[72] E.P. Sablin, R.D. Blind, I.N. Krylova, J.G. Ingraham, F. Cai, J.D. Williams, et al., Structure of SF-1 bound by different phospholipids: evidence for regulatory ligands, Molecular Endocrinology. 23 (2009) 25–34. doi:10.1210/me.2007-0508.

[73] S. Mukherjee, F.R. Maxfield, Membrane domains, Annu. Rev. Cell Dev. Biol. 20 (2004) 839–866. doi:10.1146/annurev.cellbio.20.010403.095451.

[74] A. Fujita, J. Cheng, K. Tauchi-Sato, T. Takenawa, T. Fujimoto, A distinct pool of phosphatidylinositol 4,5-bisphosphate in caveolae revealed by a nanoscale labeling technique, Proceedings of the National Academy of Sciences. 106 (2009) 9256–9261. doi:10.1073/pnas.0900216106.

Acknowledgements

I am very grateful to Professor Dr. H. Arai, lecturer Dr. Kono and assistant professor Dr. Imae for their supervisions over my 6 years of research. Also, I am grateful to associate professor Dr. T. Taguchi, assistant professor Dr. Mukai, assistant professor Dr. Ohba, Dr. M. Arita, Dr. T. Inoue and Dr. H.C. Lee for all the support in Arai lab. I thank the following researchers for providing materials and technical advices; Dr. Uchiyama and Dr. Hirano (the University of Tokyo), Dr. J. Ogawa (Kyoto University). I would like to express my gratitude to Dr. Matsuda, Dr. R. Tanaka, Dr. Ariyama, Mr. Shimanaka, Mr. S. Lee, Ms. Mao, Mr. Tokumaru and all the member of Arai lab for helpful and exciting discussions and their encouragement. I gratefully acknowledge technical assistance from Mrs. Hirata, Mrs. Akimura, Mrs. Takada. Finally, I would like to offer special thanks to my family for their supports.

January 8, 2016